Clonal evolution in serially passaged *Cryptococcus neoformans* x *deneoformans* hybrids reveals a heterogenous landscape of mitotic recombination

Lucas A. Michelotti*,[1]

Sheng Sun†

Joseph Heitman†

Timothy Y. James*

*Department of Ecology and Evolutionary Biology

University of Michigan

Ann Arbor, MI 48109 U.S.A.

†Departments of Molecular Genetics and Microbiology, Medicine, and Pharmacology and Cancer Biology

Duke University Medical Center

Durham, NC 27710 U.S.A.

[1]Current address:

Department of Entomology

University of Georgia

Athens, GA 30606 U.S.A.

Raw sequence data has been deposited into NCBI's SRA archive under BioProject: PRJNA700784, with the accession numbers SRX10055646-SRX10055684.

Running title: Lab evolution of hybrid yeast

Key words: polyploid hybrid, trisomic, experimental evolution, evolve and resequence, *Galleria mellonella*

Correspondence:

Timothy Y. James

1105 N. University

4050 Biological Sciences Bldg.

University of Michigan

Ann Arbor, MI 48109 U.S.A.

Email: tyjames@umich.edu

Abstract

Cryptococcus neoformans x *deneoformans* hybrids (also known as serotype AD hybrids) are basidiomycete yeasts that are common in a clinical setting. Like many hybrids, the AD hybrids are largely locked at the F1 stage and are mostly unable to undergo normal meiotic reproduction. However, these F1 hybrids, which display a high (~10%) sequence divergence are known to genetically diversify through mitotic recombination and aneuploidy, and this diversification may be adaptive. In this study, we evolved a single AD hybrid genotype to six diverse environments by serial passaging and then used genome resequencing of evolved clones to determine evolutionary mechanisms of adaptation. The evolved clones generally increased fitness after passaging, accompanied by an average of 3.3 point mutations and 2.9 loss of heterozygosity (LOH) events per clone. LOH occurred through nondisjunction of chromosomes, crossing over consistent with break-induced replication, and gene conversion, in that order of prevalence. The breakpoints of these recombination events were significantly associated with regions of the genome with lower sequence divergence between the parents and clustered in subtelomeric regions, notably in regions that had undergone introgression between the two parental species. Parallel evolution was observed, particularly through repeated homozygosity via nondisjunction, yet there was little evidence of environment-specific parallel change for either LOH, aneuploidy, or mutations. These data show that AD hybrids have both a remarkable genomic plasticity and yet are challenged in the ability to recombine through sequence divergence and chromosomal rearrangements, a scenario likely limiting the precision of adaptive evolution to novel environments.

Introduction

Hybridization reunites genomes of shared ancestry that diverged via speciation. Speciation generates divergent populations with fixed nucleotide differences as well as usually

64 larger-scale genomic changes such as chromosome rearrangements. Typically, hybridization
65 generates individuals of low fitness due to genetic incompatibilities in the merging genomes,
66 such as Dobzhansky-Muller genic interactions displaying negative epistasis (Orr and Turelli
67 2001; Mallet 2007). If structural differences exist between the chromosomes of the hybridizing
68 genomes, they may impair proper meiosis and lead to full or partial sterility. Overall, there exists
69 a general relationship between genetic divergence, genome rearrangements, hybrid fitness, and
70 reproductive isolation that is still poorly understood (Comeault and Matute 2018).
71 On the other hand, hybridization has the potential to facilitate adaptive evolution by
72 bringing together novel allele combinations across loci that may produce novel phenotypes.
73 Hybrid phenotypes may be transgressive or outside the bounds of parental phenotypes
74 (Rieseberg *et al.* 1999; Dittrich-Reed and Fitzpatrick 2013). Particularly in plants, hybridization
75 has led to the formation of new species, often through mechanisms such as allopolyploidization
76 which avoids the sterility barrier concomitant with chromosomal rearrangements (Rieseberg
77 2001).
78 Hybridization in fungi is increasingly recognized as having contributed to evolutionary
79 novelty and host-range expansion (Schardl and Craven 2003; Marcet-Houben and Gabaldón
80 2015; Stukenbrock 2016; Samarasinghe *et al.* 2020a). However, there are many examples of
81 fungal hybrids that appear to be restricted to the F1 diploid stage, such as the extremophile
82 *Hortaea warneckii* (Gostinčar *et al.* 2018), *Epichlöe* endophytes (Saikkonen *et al.* 2016),
83 *Aspergillus latus* (Steenwyk *et al.* 2020), and emerging pathogenic *Candida* spp. (Pryszcz *et al.*
84 2015; Schröder *et al.* 2016; Mixão and Gabaldón 2020). Because many fungi have the ability to
85 reproduce asexually for extended numbers of generations, the F1 hybrid genotypes/species
86 may generate transient, successful clonal lineages that avoid segregation load and
87 chromosomal incompatibilities that may come with meiosis (Mallet 2007). Moreover, the
88 heterosis that occurs in F1 hybrids might be particularly common, because multiple mechanisms

89 can contribute to it, such as complementation of recessive, mildly deleterious alleles,
90 overdominance, and epistasis (Shapira *et al.* 2014).
91 Despite the potential for overall heterosis in F1 hybrids, it is likely that such hybrid
92 genotypes contain a number of alleles or allelic interactions that reduce fitness, such as
93 incompatibilities driven by negative epistasis, underdominance, or gene copy number
94 imbalance. Given this situation, it is also likely that hybrids could undergo minor adaptive
95 changes in genotype through a process generally referred to as loss of heterozygosity (LOH),
96 which would allow genotypic change without wholesale meiotic shuffling. LOH during mitotic
97 divisions occurs through a number of mechanisms, including gene conversion, nondisjunction,
98 deletions, or crossing over (St Charles *et al.* 2012; Symington *et al.* 2014). The dependence on
99 sequence similarity for homology-based recombination, such as the classical double strand
100 break repair pathway (DSBR) leads to an association between crossover locations in meiotic
101 and mitotic recombination with regions of high sequence similarity (Datta *et al.* 1997; Opperman
102 *et al.* 2004; Seplyarskiy *et al.* 2014; Hum and Jinks-Robertson 2019). Overall, while it is clear
103 that asexual F1 hybrids are commonly observed in fungi, it is unclear whether asexual hybrids
104 can persist for a long time due to Muller's Ratchet (Gabriel *et al.* 1993) and by what means they
105 utilize their allelic diversity for adaptation via mitotic recombination.
106 *Cryptococcus* is a model basidiomycete yeast that causes opportunistic infections
107 particularly in immunocompromised hosts. Most infections result from colonization by *C.*
108 *neoformans* (serotype A) with infection by *C. deneoformans* (serotype D) rare (Cogliati 2013).
109 These two species are diverged by ~24.5 mya (Xu *et al.* 2000b). In both clinical and
110 environmental settings, a large percentage (~8%) of *Cryptococcus* isolates are hybrid strains,
111 particularly those formed between *C. neoformans* and *C. deneoformans*, often referred to as AD
112 hybrids (Samarasinghe and Xu 2018). Studies with AD hybrids show variable virulence and
113 hybrid vigor relative to parental species, however, evidence for transgressive segregation in
114 pathogenicity relevant traits such as resistance to UV irradiation, growth at 37 C, and resistance

115 to antifungal drugs has been observed (Litvintseva *et al.* 2007; Lin *et al.* 2008; Vogan *et al.*
116 2016; Samarasinghe *et al.* 2020a).

117 Genomic plasticity is apparent in AD hybrids, but it is unclear which mechanisms are
118 most important for adaptation. Most AD hybrids are close to diploid and, although they produce
119 sexual spores, these appear to have been produced by an aberrant form of meiosis (Lengeler *et*
120 *al.* 2001; Sun and Xu 2007; Hu *et al.* 2008; Samarasinghe *et al.* 2020b). The two parental
121 genomes are 85-90% divergent at the sequence level, and they are known to have karyotype
122 differences (Kavanaugh *et al.* 2006; Sun and Xu 2009). However, heterozygosity of AD hybrids
123 could facilitate genetic and phenotypic plasticity through genomic rearrangements or LOH
124 (Bennett *et al.* 2014; Samarasinghe *et al.* 2020a). Genomic scale studies have demonstrated
125 that naturally occurring AD hybrids typically have LOH of entire chromosomes (Hu *et al.* 2008; Li
126 *et al.* 2012; Rhodes *et al.* 2017), and there is some evidence of bias in which species
127 homologue is retained, though it is unclear what mechanism underlies this bias (Sun and Xu
128 2007; Hu *et al.* 2008; Samarasinghe *et al.* 2020b). Little is known about the extent to which
129 more spatially restricted forms of LOH, such as gene conversion and mitotic crossing over have
130 contributed to LOH in natural AD hybrids. A recent experimental evolution study of an AD hybrid
131 genotype showed that LOH of Chr. I could be rapidly stimulated if hybrids were grown in the
132 presence of the antifungal fluconazole, which has a strong resistance allele encoded on Chr. I of
133 the *C. neoformans* parent (Stone *et al.* 2019; Dong *et al.* 2020). In this same study, LOH was
134 shown to occur at a rate of 6×10^{-5} per locus per mitotic division, and the distribution of LOH
135 was unequal across chromosomes. The precise mechanisms of LOH in this and other studies
136 are masked due to low numbers of markers utilized, making it altogether unclear whether the
137 high level of sequence diversity could reduce the potential for homologous recombination during
138 repair of DSB through anti-recombination mechanisms. It was recently demonstrated that
139 deletion of the DNA mismatch repair gene *MSH2* did not increase the rate of homologous
140 recombination in meiotic progeny of an AD hybrid cross as observed in most other species but

141 did increase viability through increased aneuploidy, a result consistent with either sequence
142 dissimilarity or genetic incompatibility limiting recombination in *Cryptococcus* AD hybrids (Priest
143 *et al.* 2021).
144 In this study, we experimentally evolved AD hybrids to six distinct environments in order
145 to test which mechanisms of genomic change are involved in rapid adaptation. Using replicate
146 populations, both in liquid media and a model host (larvae of the waxworm moth *Galleria*
147 *mellonella*), we tested for evidence of parallel mutation, LOH, or copy number variation across
148 genes and chromosomes. Because of the divergence between parental alleles, we
149 hypothesized that unlike in *Candida albicans* (Ene *et al.* 2018) and *Saccharomyces cerevisiae*
150 (James *et al.* 2019) LOH would primarily be through nondisjunction of entire chromosomes
151 rather than via mechanisms that involve homologous recombination (e.g., gene conversion or
152 crossing over). Finally, we designed the experiment so that it would test whether particular
153 environments would favor one parental genotype than the other as previous investigations have
154 hinted at (Hu *et al.* 2008; Samarasinghe *et al.* 2020b).
155
156 **Materials and Methods**
157
158 *Strains*
159 We initiated evolution starting with a single diploid hybrid strain generated by crossing *C.*
160 *neoformans* haploid strain YSB121 (KN99 *MAT***a** *aca1::NEO ura5 ACA1-URA5*) with *C.*
161 *deneoformans* strain SS-C890 (*MAT*α *NAT* ectopically inserted into a JEC21 genome and later
162 determined to be inserted in the sub-telomeric region of the left arm of Chr. 1). Over 100 diploid
163 products resistant to NAT and G418 were identified that also produced extensive filamentation
164 on V8 agar, and these were genotyped at 11 PCR markers across 6 chromosomes plus the
165 *MAT* locus (**Suppl. Table 1**) to identify highly heterozygous diploid offspring. The genotypes of
166 these markers were determined by size differences or presence/absence of a band (*STE20*

167 locus) using agarose gel electrophoresis. One of the diploids (SSD-719) heterozygous at all
168 markers was chosen as the ancestor for both *in vivo* and *in vitro* passaging. A near isogenic
169 strain (SSE-761) was generated to serve as a reference competitor strain by random integration
170 of a GFP-Nop1::*HYG* cassette into SSD-719 (Park *et al.* 2016).
171
172 *Passaging in vitro*
173 Experimental passaging in five media types followed James et al. (2019). Briefly, 8 replicate
174 populations of 500 μl were inoculated with the hybrid ancestor strain, grown at 30 °C with
175 shaking, and transferred daily with 1/50 dilution. The media types were yeast peptone dextrose
176 (YPD), beer wort, wine must, YPD + high salt (1 M NaCl), and minimal medium plus canavanine
177 (James *et al.* 2019). Every fifth passage, 25 μl of each population was subsampled for archiving
178 in 25% glycerol at -80 °C. At the end of 100 days, one clone was isolated from each population
179 by streak plating, and the remaining population archived.
180
181 *Passaging in vivo*
182 We utilized last instar larvae of *Galleria mellonella* for the infection model with inoculation and
183 incubation following (Phadke *et al.* 2018). Six replicate populations of 5 larvae were founded,
184 with each larva injected with 10^7 cells. Larvae were incubated 5 days with ambient temperature
185 and lighting. The larvae were then crushed in 50 ml sterile water and 50 μl were plated onto
186 three 15 cm plates of YPD containing 200 mg/L G418 and 200 mg/L ampicillin. After 72 hr of
187 incubation, the plates containing on the order of 10^3-10^4 small colonies were scraped and
188 pooled into 50 ml of sterile water, the concentration adjusted to the appropriate level 10^6/μl for
189 inoculation, and the next population of 5 larvae was inoculated. After 10 passages in this
190 manner, a single clone from each population was isolated for analysis.
191

192 *Fitness estimation*

193 We estimated fitness of our evolved strains using both growth curves and competition with a
194 reference strain. Growth curves were estimated using a Bioscreen C (Growth Curves USA)
195 following James et al. (2019). Competition-based fitness was measured by comparing
196 proportions of unlabeled cells (evolved) with a near isogenic competitor strain (SSE-761)
197 engineered to express GFP. Mixtures of the competitor strain and evolved strain were analyzed
198 for green fluorescent events to non-fluorescent events both before and after growth on a iQue
199 Screener PLUS (Intellicyt) according to James et al. (2019). Each pairwise competition was run
200 using 8 replicate populations.

201

202 Fitness and virulence was also estimated in the *Galleria*-passaged clones as well as two clones
203 isolated from beer wort. Virulence was estimated by survivorship of 10 larvae following injection
204 of 10^6 cells per larva. Virulence for each strain was measured as the daily survivorship of larvae
205 up to one week post-inoculation. *In vivo* fitness of the evolved strains was estimated by co-
206 injection of evolved with competitor strain SSE-761 as a combination of 2 x 10^6 cells in 10 μl into
207 each of 5 larvae. After incubation for 48 hrs, larvae were crushed in sterile water, filtered
208 through a 40 μm filter, and plated on two media types: YPD media containing G418 (200 mg/L),
209 ampicillin (200 mg/L), and chloramphenicol (25 mg/L), and YPD media containing the same
210 antibiotics plus hygromycin (200 mg/L) and incubated at 30 °C until colony development. The
211 latter media type only permits growth of the competitor strain while the former allows growth of
212 both evolved and competitor. All experiments were repeated three independent times. Colony
213 sizes varied considerably, and in order to count the colonies in a rapid, objective manner, we
214 used the program OpenCFU (Geissmann 2013) using a threshold of 5 and a minimum radius of
215 20. All fitness (F) values were calculated using colony counts on G418-only media pre- (G_{pre})

216 and post-injection (G_{post}) and colony counts on G418+hygromyin media pre- (H_{pre}) and post-
217 injection (H_{post}) using the following formula:

218 $$F = \frac{G_{post}/H_{post}}{G_{pre}/H_{pre}}$$

219 We presented *F* as mean relative fitness across the replicates by division by the mean *F*
220 estimate for the ancestral genotype vs. congenic competitor strain.
221
222 *Genome resequencing*
223 DNA was extracted from clones grown overnight in 2 ml of YPD following (Xu *et al.* 2000a). One
224 clone from each population was sequenced, for a total of 35 clones (library of CB-100-4 failed to
225 pass QC). The ancestral haploid and diploid parents were also sequenced. Because the clones
226 evolved via passaging in *Galleria* were initiated after the *in vitro* evolution experiment using a
227 separate ancestral subclone, we also sequenced the two ancestral diploid genotypes
228 separately. Libraries for genome sequencing were constructed with dual indexing using 0.5-2.5
229 ng per reaction using a Nextera XT kit (Illumina). The libraries were multiplexed and sequenced
230 on an Illumina HiSeq 2500 v4 or NextSeq sequencer using paired end 125 bp output. After
231 analyses the actual coverage for each strain ranged from 41-147X.
232
233 *Data analyses*
234 The full pipeline, including scripts and data sets used for analysis of the genomic data can be
235 found at https://github.com/Michigan-Mycology/Cryptococcus-LOH-paper, with larger variant call
236 format (vcf) files stored using figshare. Details of the variant calling pipeline using GATK 4.0.0
237 (McKenna *et al.* 2010) are similar to James et al. (2019). Briefly, data were trimmed for quality
238 using Trimmomatic 0.36 (Bolger *et al.* 2014). The genomes of the two parental haploid strains
239 backgrounds (JEC21 (Loftus *et al.* 2005), H99 (Janbon *et al.* 2014)) were downloaded and
240 aligned using Harvest (Treangen *et al.* 2014). The variants from these alignments were used as

241 a set of known variants in the base recalibration step of GATK. SNP identification was
242 conducted using HaplotypeCaller using the H99 genome as the reference. After variant filtration
243 for quality in GATK, SNPs were converted into a vcf file and further filtered. Genotypes were set
244 to unknown when their depth was < 18X or > 350X, the genotype quality (GQ) was < 99, or the
245 sites were not present as differences between the haploid ancestors observed as
246 heterozygosity in the diploid ancestor. SnpEff 4.3k (Cingolani *et al.* 2012) was used to assign
247 functional information to SNPs. We scanned for new mutations occurring during passaging
248 using the criteria that they were absent in both haploid parents and ancestral diploid strain and
249 appeared with sequencing depth > 18X and GQ >= 99. Estimating the number and length of
250 each LOH event was done using the custom perl script
251 calculate_LOH_lengths_crypto_100_new.pl. After identifying LOH patterns, we later verified
252 each event by examining the read pileup and vcf file and excluded LOH events which were not
253 supported by 100% of reads as homozygous. We removed single SNP LOH events, because
254 they showed strong association of reads linked to only a single allele in flanking heterozygous
255 SNPs, indicating they are likely false positives. Indels were ignored for considering LOH, which
256 underestimates the overall amount of LOH and allelic diversity, but should not cause systematic
257 biases in hypothesis testing.
258
259 We identified aneuploidy using chromosome specific coverage estimated with bedtools v. 2.29.2
260 (Quinlan and Hall 2010). Aneuploidy was considered when read depth < 0.65 or > 1.35 the
261 genome-wide average (Zhu *et al.* 2016). Local scale copy number variation (CNV), specifically
262 looking for deletions, was evaluated using the software smoove
263 (https://github.com/brentp/smoove).
264

265 All statistical analyses and plots were conducted in R 3.6.2 (R_Core_Team 2019) unless
266 otherwise specified. Most statistical tests utilized the base package; we also utilized the
267 functions ggplot2 (Wickham 2009) and gridextra for graphical output (Auguié 2017).
268
269 *Data availability*
270 Strains and plasmids are available upon request. The full pipeline, including scripts and data
271 sets used for analysis of the genomic data, additional data files, and code for reconstructing
272 figures can be found on Github (https://github.com/Michigan-Mycology/Cryptococcus-LOH-
273 paper). Raw sequence data has been deposited into NCBI's SRA archive under BioProject:
274 PRJNA700784, with the accession numbers SRX10055646-SRX10055684.
275
276 **Results**
277
278 *Evidence for adaptation during passaging*
279
280 We evolved a single AD hybrid genotype (SSD-719) in 5 *in vitro* environments by serial transfer
281 for 100 days and also evolved the genotype through 10 serial passages in waxworm larvae.
282 Each environment was represented by 6 replicate populations, and from each of these evolved
283 populations we isolated individual clones, determined whether they had evolved a higher fitness
284 relative to the ancestral genotype, and sequenced their genomes. The 6 clones isolated after
285 evolution in each *in vitro* environment generally showed increased fitness relative to the
286 ancestral genotype (**Figure 1**). Maximal population density (EOG) and competitive fitness
287 mostly increased for all strains and environments, whereas doubling time was lower for clones
288 evolved in high salt or canavanine environments.
289

290 The virulence and relative fitness of the *G. mellonella* passaged strains was estimated for the 6
291 clones that had been serially passaged 10 times in the same host compared with the ancestral
292 diploid genotype and isolates that had been evolved in beer wort. The larval passaged strains
293 showed no evidence of increased virulence (**Suppl. Figure 1**); however, they showed enhanced
294 survivorship (one-way ANOVA, [F(8,18)=3.59, P=0.0115]) compared to the beer wort evolved
295 and ancestral strain as measured by genotype recovery after co-injection with a marked strain
296 (**Figure 2**).
297
298 *Rate and spectrum of LOH*
299
300 LOH was readily apparent at the chromosome scale (**Figure 3**), suggesting that most strains
301 had undergone chromosome-scale LOH events as well as numerous smaller events. We
302 estimated that strains had undergone an average of 2.9 LOH events after 100 days,
303 encompassing an average of 2.26 Mbp. There was a significant difference between the average
304 number of LOH events across environments (Kruskal-Wallis test, $X^2(5) = 18.26$, $p = 0.026$), but
305 these differences were driven mostly by low LOH numbers in larval passaged strains (beer wort:
306 2.8, canavanine: 4.2, high salt: 1.8, wine must: 2.7, YPD: 4.7, larvae: 0.8). Most of the LOH
307 events were the result of whole chromosome events, with the second most common being long
308 distance LOH consistent with BIR observed as crossing over not associated with gene
309 conversion, followed by gene conversion, and then deletions (**Figure 4**). Crossover events
310 averaged 173 kb in total length, and gene conversions averaged 7.4 kb.
311
312 Using the rate of LOH events uncovered and their sizes, we estimated a rate of 0.005
313 events/generation, 4.0 kb/generation, and 2×10^{-4} per bp per generation. Dong et al. (2019)
314 estimated a rate of LOH of 6×10^{-5} per locus per mitotic division with 33 loci in *Cryptococcus* AD

315 hybrids, leading to an estimation of 0.002 LOH events per generation. The higher level in our
316 study is likely due to a higher detection level using NGS.
317
318 *Evidence for aneuploidy and copy number variation (CNV) after passaging*
319
320 Aneuploidy leading to CNV is a rapid means of generating adaptive genetic variation in
321 pathogenic fungi (Bennett *et al.* 2014; Beekman and Ene 2020). We tested for the presence of
322 both whole chromosomal and partial chromosomal aneuploidy by using density of reads
323 mapped to the genome. We found that the evolved strains showed aneuploidy on multiple
324 chromosomes (**Suppl. Figure 2**). In all cases, aneuploidies were trisomies and no evidence of
325 whole chromosome monosomies was found. Particular chromosomes (Chr. 2, 4, 9, and 10)
326 were likely to display aneuploidy, but in some cases the aneuploidy was present in ancestral
327 diploid genotypes. For example, Chr. 9 was trisomic in all larval passaged clones, but was also
328 observed in the *in vivo* diploid ancestor, although most passaged strains maintained
329 heterozygosity on Chr. 9 unlike the ancestor.
330
331 Inspection of coverage across strains was used to confirm aneuploidy (**Suppl. Figures 3-6**).
332 Aneuploidies were strikingly associated with the same chromosomes that had also undergone
333 whole chromosome LOH (**Figure 3**), however, in general, trisomic chromosomes typically
334 retained both parental homologues. For example, clones CW-100-6, CY-100-3, CY-100-6,
335 P3W10, P6W10 showed partial or complete trisomy for Chr. 2 (**Suppl. Figures 4-5**), and these
336 are precisely the strains that have not undergone whole chromosome LOH at Chr. 2 (**Figure 3**).
337 Instead these strains apparently have two partial or complete copies of the *C. deneoformans*
338 homolog and one *C. neoformans* homolog based on allele frequencies, suggesting that two
339 copies of *C. deneoformans* Chr. 2 is strongly favored in the hybrid genotypes. Chromosome
340 plots and a structural variant detection method (smoove) were also employed to detect partial

341 aneuploidy occurring via partial chromosomal deletion. Six LOH events were consistent with
342 deletions (2 identified by smoove and 4 visually from relationship of coverage with LOH events),
343 4 of which were sub-telomeric. Overall, these data suggest that particular aneuploidies are not
344 consistently observed in an environment or associated with LOH, but aneuploidy is nonetheless
345 widespread and can be stably maintained for many clonal generations.
346
347 *Identification of point mutations after passaging*
348
349 We found 117 high quality *de novo* mutations at 93 SNP loci specifically occurring in the
350 evolved clones that were absent from both haploid and diploid ancestors. The mean number of
351 mutations per strain was 3.3 (range 0-10). The majority of the mutations were inside exons
352 (85%), with the remaining intronic (11%), or in the 5' untranslated region of genes (4%). Most of
353 the mutations in exons had consequences on the protein sequence, with 63.3% missense, 6.3%
354 nonsense, and 30.4% synonymous. One mutation was expected to abolish proper intron
355 splicing by removal of the intron acceptor sequence. The mutations were found on each of the
356 14 chromosomes. Of 117 mutations only 4 of them were found as homozygous genotypes.
357 Because a number of chromosomes have undergone whole chromosome or long distance LOH,
358 the fact that most mutations are heterozygous implies that whole chromosome LOH likely
359 occurred early on during the evolution of the populations, followed by mutations.
360
361 Mutations with protein-altering effects were found in diverse genes, including transcription
362 factors, plasma-membrane proton-efflux P-type ATPase, and many others. A test for enrichment
363 of Gene Ontology terms among the protein-altering mutations using clusterProfiler (Yu *et al.*
364 2012), identified lipid metabolic process as the most enriched term (uncorrected P = 0.003),
365 although this enrichment is not statistically significant after correction for multiple testing (FDR
366 corrected P = 0.103).

367

368 *Parallel evolution occurred primarily as whole chromosomal events skewing evolved clones*
369 *towards one parental genotype*

370

371 We looked for evidence that specific LOH events and point mutations showed parallel evolution
372 across independently evolved clones. We specifically noted parallel changes as regions of the
373 genome undergoing LOH or mutation in 3 or more clones. Among the LOH events, 11 were
374 found in more than 3 clones, including whole chromosome or long distance LOH on Chr. 2, 4, 9
375 and 12 (**Figure 3**). The other regions were limited to only 3 clones. There was no evidence for
376 any of the LOH events being more predominant in particular environments. Of the 93 *de novo*
377 single nucleotide mutation loci, only 3 were found in 3 or more strains. Three loci showed 3, 7,
378 and 8 strains bearing the mutation. These were all mutations of low impact and may represent
379 variation in the initial founding population that became fixed during evolution.

380

381 We then asked whether whole-chromosome LOH events favored one parental type over
382 another, which was obvious for Chr. 2 in which LOH exclusively led to retention of the *C.*
383 *deneoformans* homolog. For the 4 chromosomes (2, 4, 9 and 12) with 4 or more independent
384 LOH events we tested whether the allelic distribution of homozygotes was non-random or
385 skewed towards one parent. Although events at most chromosomes favored one parental
386 genotype over another, only the Chr. 2 pattern was significant (P=8.2e-06; Fisher's exact test).

387

388 We then tested whether one of the parental genotypes was globally favored over the other
389 across isolates by asking whether the ratio between SNP loci that are homozygous of the
390 *neoformans* and *deneoformans* alleles, respectively, deviated significantly from a random 1:1
391 null hypothesis. Overall, we found that the mean frequency of *neoformans* alleles in LOH
392 regions across all evolved clones was 0.234 (CI: 0.115-0.353), which was significantly different

393 from the null hypothesis (t(34) = -4.61, p = 7.0e-5). However, if Chr. 2 was excluded, the mean
394 frequency of *neoformans* alleles in LOH regions was 0.639 (CI: 0.488-0.791), which was not
395 significantly different from the null expectation ($t(34) = 1.88$, $p = 0.070$). These data suggest
396 there is no signal of a favored parental allele arising from the LOH process with the exception of
397 LOH favoring retention of the *C. deneoformans* Chr. 2 homolog.
398
399 *Relationship of LOH break points to sequence divergence and mutation*
400
401 The ability to undergo crossing over could be influenced by anti-recombination mechanisms that
402 prohibit recombination due to sequence divergence. Such a mechanism would favor
403 recombination breakpoints in regions of lower divergence. We found no relationship between
404 heterozygosity of particular chromosomes and the number of crossover events observed (r(12)
405 = 0.083, p = 0.78; **Suppl. Table 2**). By plotting the locations of mitotic recombination
406 breakpoints and mutations relative to chromosomal divergence (**Figure 5**), we identified a clear
407 pattern that many of the breakpoints are sub-telomeric, and sub-telomeric regions often have
408 lower divergence between the two parents. We tested whether the heterozygosity near crossing
409 over breakpoints was depressed relative to random breakpoints produced in simulated data
410 sets. In total there were 47 independent breakpoints observed (only the left breakpoint was
411 used for gene conversion events). For windows of size 1000 bp centered around the
412 breakpoints, the mean post-filtering heterozygosity of the windows was 0.026. From 1000
413 simulated data sets, the mean simulated divergence near random breakpoints was much higher
414 (0.045), with a range of 0.037-0.051, providing a highly significant (P<0.001) difference between
415 heterozygosity near observed breakpoints to randomly chosen ones. Varying the window size
416 from 30-10^5 bp revealed that heterozygosity near LOH breakpoints was lower than the random
417 expectation for every case (P<0.001). This result suggests that recombination in *Cryptococcus*
418 AD hybrids is favored in broad regions of lower divergence between recombining genomes.

419

420 In *Candida albicans*, a positive relationship has been observed between mitotic recombination
421 and *de novo* mutation (Ene *et al.* 2018), indicative of recombination-induced mutagenesis as
422 observed in meiosis in yeast and other organisms (Arbel-Eden and Simchen 2019). We tested
423 for such a relationship by comparing the relative distance of observed mutations to crossover
424 locations to a simulated set of random mutations in the genome (1,000 simulations). This result
425 supports the overview in **Figure 5** that suggests there is no clear relationship between *de novo*
426 mutation and crossover events in *Cryptococcus* AD hybrids (P = 0.508).

427

428 **Discussion**

429

430 Mutations are the primary way in which clonal organisms evolve. However, there are additional
431 avenues for genetic change in clonal organisms referred to as genome plasticity, which are
432 particularly available to polyploid hybrid genomes (Albertin and Marullo 2012; Blanc-Mathieu *et*
433 *al.* 2017; Samarasinghe *et al.* 2020a). In this study we investigated the sources of genetic
434 variation in evolving hybrid strains of *Cryptococcus* continuously passaged in differing
435 environments. Passaging led to adaptation as observed by increased fitness of the clones
436 isolated at the end of the experiment relative to the ancestral genotype. Both genome plasticity
437 and *de novo* mutation were identified in the evolved clones via genome resequencing. Genomic
438 plasticity was observed as chromosome copy number amplification and LOH generated via
439 nondisjunction, gene conversion, and crossing over. However, the location of these genome
440 scale events is highly biased across the genome, occurring in particular chromosomal locations
441 presumably deeply influenced by the history of the divergence of the two sibling species.

442

443 This experiment was conducted at the same time as a similar passaging experiment using
444 *Saccharomyces cerevisiae* (James *et al.* 2019), and therefore the media conditions were

445 atypical for *Cryptococcus*. Therefore, it is unsurprising that the *Cryptococcus* hybrid genotype
446 improved significantly in fitness over the period of evolution, particularly as measured by density
447 at carrying capacity (EOG) and in head-to-head competition with the ancestor (**Figure 1, B-C**).
448 Gains in fitness across environments were more consistent than the comparable *S. cerevisiae*
449 evolved populations, but the reason for these differences in the fitness landscape for the two
450 species is uncertain. It may be that *S. cerevisiae* evolution was more influenced by strong
451 genotype by environment interactions or the low fitness of the F1 genotypes of AD hybrids may
452 have facilitated rapid fitness gains regardless of environment.
453
454 *Cryptococcus* AD hybrids had a lower average LOH rate (2.9 event/100 days) relative to *S.*
455 *cerevisiae* (5.2 events/100 days), despite the same dilution rate on transfer and hence
456 equivalent number of generations. Moreover, the mechanism of LOH in *Cryptococcus* AD
457 hybrids was very different than that of *S. cerevisiae* heterozygous diploids. Specifically, LOH in
458 *Cryptococcus* is dominated by nondisjunction of chromosomes, while LOH in *S. cerevisiae* had
459 gene conversion as the majority mechanism and no evidence of whole chromosome LOH. Both
460 fungi had LOH consistent with crossing over or BIR (**Figure 4**; Class 4), but *S. cerevisiae* had
461 considerably more crossing over associated with gene conversion, consistent with the classical
462 double strand break repair model (Symington *et al.* 2014). A major difference that may explain
463 this pattern is that the initial heterozygosity of the ancestral diploid genotypes of *Saccharomyces*
464 was 0.005-0.009 or one heterozygous position out of every 100. In our highly filtered
465 *Cryptococcus* data set, we considered 5.6e05 heterozygous positions in the AD hybrids (0.03
466 heterozygosity), however, it is known that *C. neoformans* and *C. deneoformans* are 85-90%
467 divergent at the sequence level (Kavanaugh *et al.* 2006; Sun and Xu 2009) making differences
468 on the order of 10 bases for every 100.
469

470 LOH locations are highly heterogeneous across the *Cryptococcus* genome. Whole chromosome
471 LOH was primarily observed on chromosomes 2, 4, and 9. Crossover locations were highly
472 biased towards sub-telomeric regions, and these are regions where there are fewer
473 heterozygous mapped positions. It is worth pointing out, however, that there are multiple
474 explanations for lower heterozygosity at the telomeric regions. One could be hemizygosity at
475 these regions, or the known enrichment of repetitive DNA elements such as transposons (Loftus
476 *et al.* 2005), which remain unmapped with short read technology. Comparison of *C. neoformans*
477 to *C. deneoformans* has identified 32 chromosomal rearrangements (Sun and Xu 2009). Most of
478 these are smaller inversions or complex rearrangements, while a few of them represent large
479 chromosomal changes, such as multiple translocations and inversions between chromosomes 3
480 and 11. The rearrangement between Chr. 3 and 11 has a severe and suppressive impact on
481 long distance LOH both as whole chromosome loss or as crossover events. Other larger
482 chromosomal rearrangements likely had additional suppressive effects on the ability of the
483 homologous chromosomes to undergo mitotic recombination. For example, no crossover events
484 were observed on the right arm of chromosome 9, which is expected due to the large inversion
485 between *C. neoformans* and *C. deneoformans* in this region (Sun and Xu 2009).
486
487 If sequence dissimilarity and chromosome rearrangements hinder mitotic recombination what
488 might stimulate it? It is clear that there is an association between transposable elements and
489 chromosomal rearrangement and introgression (Kavanaugh *et al.* 2006; Sun and Xu 2009). Two
490 regions of the *Cryptococcus* genome have been identified where ancestral introgression likely
491 occurred between the two parental lineages (Kavanaugh *et al.* 2006). The smaller of these
492 events encompasses ~12 kb of the left arm of *C. neoformans* Chr. 10 which is found on the right
493 arm of Chr. 13 in *C. deneoformans*. This small region of ~5% sequence divergence harbored 3
494 of the 47 independent breakpoints. The second, larger introgression event is a 40 kb region
495 found in a sub-telomeric region of the left arm of *C. neoformans* Chr. 5 which was apparently

496 the parent of a non-reciprocal introgression and translocation into *C. deneoformans*. Strikingly,
497 4/6 non-whole chromosome LOH events occurring on *C. neoformans* Chr. 5 have a crossover
498 event in this "identity island". Two of these events are gene conversions with one end near the
499 boundary of the island where one partial copy of the non-LTR retrotransposon Cnl1 is present.
500 These results allude to a scenario in which the transposable elements both speed up and slow
501 down the speciation process. Between isolated populations, transposition of elements can
502 cause genomic rearrangements that inhibit normal meiosis upon secondary contact (Sun and
503 Xu 2009; Zanders *et al.* 2014; Serrato-Capuchina and Matute 2018). However, transposable
504 elements could also facilitate the cohesion of populations by facilitating introgression, which in
505 turn increases the number of opportunities for recombination via mitotic recombination and gene
506 conversion in hybrids.
507
508 While this experiment played out over a mere ~500 generations, naturally occurring hybrids
509 reveal evolutionary processes occurring over much longer time periods. *Cryptococcus* AD
510 hybrids have arisen multiple times independently and may have undergone clonal evolution for
511 up to 2 million years (Xu *et al.* 2002; Litvintseva *et al.* 2007). The results in our microevolution
512 study show many similarities to genomic analysis of the natural hybrids. For example, all studies
513 have observed both whole chromosome LOH and aneuploidy via chromosomal amplification,
514 and monosomy is not tolerated, meaning the lost copy of a chromosome is duplicated from the
515 remaining copy to restore diploidy, or alternatively that duplication of one homolog precedes
516 loss (Hu *et al.* 2008; Sun and Xu 2009; Li *et al.* 2012; Rhodes *et al.* 2017). The specific
517 chromosomes involved, however, are different. All studies reported loss of the *C. deneoformans*
518 Chr. 1 copy in some strains (Hu *et al.* 2008; Sun and Xu 2009; Li *et al.* 2012; Rhodes *et al.*
519 2017) which was not observed in our study. No studies showed the most common whole
520 chromosome LOH in our study of loss of *C. neoformans* Chr. 2 homolog (**Figure 3**), though a
521 partial LOH was reported (Rhodes *et al.* 2017). While there are shared whole chromosome LOH

522 events between our study and others as in loss of the C*. deneoformans* Chr. 9 homolog or loss
523 of the *MAT* encoding Chr. 4 (Sun and Xu 2009; Li *et al.* 2012; Rhodes *et al.* 2017), the general
524 pattern across strains and studies is mostly stochastic, which contrasts with the highly
525 deterministic pattern seen for Chr. 2 in our experimental population. A possible explanation is
526 that the hybridization events are independent, and all of a different background than the lab
527 generated one used in this study. Many hybrids have the VNB lineage as the *C. neoformans*
528 parent, but in our study the *C. neoformans* parent was VNI (Litvintseva *et al.* 2007; Li *et al.*
529 2012).
530
531 Genomic plasticity via LOH and aneuploidy are predicted to be adaptive, though this must be
532 contrasted with a more neutral model. In the case of drug resistance in AD hybrids aneuploidy
533 and increased copy number is clearly selected for through amplification of resistance genes (Li
534 *et al.* 2012; Rhodes *et al.* 2017; Dong *et al.* 2020). Aneuploidy may merely be a byproduct of the
535 fact that chromosomal loss or duplication is the fastest means of achieving copy number change
536 or homozygosity of a single gene. That selection was responsible for the rapid increase in
537 homozygosity of Chr. 2 to the *C. deneoformans* homolog is supported by the fitness values of
538 strains without homozygosity of the Chr. 2 *C. deneoformans* homolog. Specifically, CY-100-3
539 and CY-100-6 lacking the LOH event had the two lowest fitness values for YPD evolved strains
540 in two fitness measures (doubling time and relative fitness versus competitor). These data are
541 consistent with the strong bias towards the *C. deneoformans* parent of Chr. 2 in a large sample
542 of sexually recombined progeny from an AD hybrid of similar genetic background (Sun and Xu
543 2007), hinting that there may exist incompatibilities between genes from the two species on this
544 chromosome as predicted by the Dobzhansky-Muller model. Such intra- and inter-chromosomal
545 incompatibilities have been detected in a previous study of AD hybrids, suggesting that this a
546 plausible explanation (Vogan and Xu 2014). Alternatively, rather than epistatic interactions,
547 dosage or RNA/protein titer could differ between products encoded by the two parental

548 homologs, and this could provide opportunities for selection to act. For example, if there are
549 genes not present on Chr. 2 of *C. neoformans* that exist in *C. deneoformans* or if the expression
550 level of the *C. deneoformans* genes on Chr. 2 is more optimal, this could lead to selection
551 favoring loss of the *C. neoformans* homolog. As Chr. 2 is the chromosome containing the
552 ribosomal RNA (rRNA) array, we might hypothesize that either copy number or expression of
553 these genes could be involved in rapid whole chromosome LOH.
554
555 Although we did not find parallel mutations occurring in identical genes or types of genes, it is
556 likely that many of the mutations we observed had positive effects on fitness. For example, the
557 missense mutation observed in a larval passaged strain (P3W10) in *HSP104* (CNAG_07347), a
558 gene known to be involved in tolerance and upregulated during pathogenicity (Steen *et al.* 2003;
559 Yang *et al.* 2017) may reflect mutation favored in the larval environment. We recorded ~3
560 mutations per strain with an expected percentage of 61% moderate to high effect on protein
561 sequence, e.g., nonsense and missense. This value is similar to the expected ratio of mutational
562 types observed in clonal evolution of *S. cerevisiae* (McDonald *et al.* 2016; Fisher *et al.* 2018). In
563 experimentally passaged *in vitro* and *in vivo Candida albicans*, the authors recorded a much
564 lower rate of missense mutations which they ascribed to stronger purifying selection (Ene *et al.*
565 2018). This could be due to experimental differences. For example, in one experimental
566 passaging experiment the authors used a single clone bottleneck in between serial passages,
567 however, they artificially selected the strains with the highest virulence to continue the
568 passaging. Further work in our system needs to be done to test the effects of mutations that
569 arise during experimental infection.
570
571 Although *Galleria mellonella* has a number of advantages in its use as an experimental model, it
572 has definite weaknesses, which are apparent from this study. We found that, like *S. cerevisiae*
573 (Phadke *et al.* 2018), immediately after injecting large numbers of *Cryptococcus* cells, the host

574 is able to kill most cells based on <1% recovery of cells from crushed larvae plated onto
575 selective media (data not shown). This reduces the effective population size of passaged yeast
576 populations and provides a partial explanation for the fact that larval passaged lines had the
577 lowest LOH and mutation rates. However, our data do suggest that, unlike for *S. cerevisiae*,
578 strains passaged through waxworm larvae evolved increased ability to compete in the host
579 environment. Improvements to the model could involve immunosuppression of the host through
580 chemical treatments or modification of the environmental conditions (Torres *et al.* 2016) to favor
581 growth of *Cryptococcus*. Recovery of cells via gradient centrifugation or flow cytometry from
582 infected larvae would eliminate the growth phase in YPD thus improving the consistency of
583 selective pressure.
584
585 Overall, the contrasting results in LOH rate and mechanism between *Cryptococcus* hybrids and
586 *Saccharomyces* diploids (James *et al.* 2019; Sui *et al.* 2020) suggest that LOH in *Cryptococcus*
587 hybrids is comprised largely of whole chromosome events in part because of the inability for
588 *Cryptococcus* AD hybrids to undergo recombination. This evidence comes from the association
589 between crossover breakpoints and regions of lower heterozygosity, such as identity islands
590 shaped by introgression, an observation consistent with literature showing mitotic and meiotic
591 recombination is reduced in species with higher heterozygosity (Opperman *et al.* 2004;
592 Seplyarskiy *et al.* 2014; Hum and Jinks-Robertson 2019; Tattini *et al.* 2019). It may be, however,
593 that *Cryptococcus* has lower recombination rate overall compared to model species such as
594 *Saccharomyces* which are highly recombinogenic. For example, during experimental genetic
595 transformation the rate of homologous recombination very low *Cryptococcus* (Davidson *et al.*
596 2000). Intraspecific meiotic recombination rates have been estimated using mapping
597 populations of *C. deneoformans*, with the results comparable to *S. cerevisiae* (~5 kb/cM)
598 (Cherry *et al.* 1997; Forche *et al.* 2000; Sun *et al.* 2014; Roth *et al.* 2018). Rates of mitotic
599 recombination within *Cryptococcus* intraspecific crosses have not been measured. In our study

design, we also evolved *C. deneoformans* diploids that were completely homozygous. These homozygous diploid populations showed a similar rapid increase in fitness as evolved *Cryptococcus* hybrid clones, and future genome sequencing could resolve whether most *de novo* mutations remain heterozygous as observed in hybrid clones or may have undergone LOH at a higher rate.

Acknowledgements

This work was made possible by grants from the National Institutes of Health, National Institute of Allergy and Infectious Diseases (5R21AI105167-02, R37 AI39115-23, and R01 AI50113-16). J.H. is co-director and fellow of CIFAR program Fungal Kingdom: Threats & Opportunities. We thank Emmi Mueller and Ellen James for technical lab support.

Literature Cited

Albertin W., and P. Marullo, 2012 Polyploidy in fungi: evolution after whole-genome duplication. Proceedings of the Royal Society B: Biological Sciences 279: 2497–2509. https://doi.org/10.1098/rspb.2012.0434

Arbel-Eden A., and G. Simchen, 2019 Elevated mutagenicity in meiosis and its mechanism. BioEssays 41: 1800235. https://doi.org/10.1002/bies.201800235

Auguié B., 2017 gridExtra: Miscellaneous Functions for “Grid” Graphics. R package version 2.3. https://CRAN.R-project.org/package=gridExtra.

Beekman C. N., and I. V. Ene, 2020 Short-term evolution strategies for host adaptation and drug escape in human fungal pathogens. PLOS Pathogens 16: e1008519. https://doi.org/10.1371/journal.ppat.1008519

Bennett R. J., A. Forche, and J. Berman, 2014 Rapid mechanisms for generating genome diversity: whole ploidy shifts, aneuploidy, and loss of heterozygosity. Cold Spring Harb Perspect Med 4: a019604. https://doi.org/10.1101/cshperspect.a019604

626 Blanc-Mathieu R., L. Perfus-Barbeoch, J.-M. Aury, M. Da Rocha, J. Gouzy, *et al.*, 2017
627 Hybridization and polyploidy enable genomic plasticity without sex in the most
628 devastating plant-parasitic nematodes. PLoS Genet 13: e1006777.
629 https://doi.org/10.1371/journal.pgen.1006777
630 Bolger A. M., M. Lohse, and B. Usadel, 2014 Trimmomatic: a flexible trimmer for Illumina
631 sequence data. Bioinformatics 30: 2114–2120.
632 https://doi.org/10.1093/bioinformatics/btu170
633 Cherry J. M., C. Ball, S. Weng, G. Juvik, R. Schmidt, *et al.*, 1997 Genetic and physical maps of
634 Saccharomyces cerevisiae. Nature 387: 67–73.
635 Cingolani P., A. Platts, L. L. Wang, M. Coon, T. Nguyen, *et al.*, 2012 A program for annotating
636 and predicting the effects of single nucleotide polymorphisms, SnpEff: SNPs in the
637 genome of Drosophila melanogaster strain w(1118); iso-2; iso-3. Fly 6: 80–92.
638 https://doi.org/10.4161/fly.19695
639 Cogliati M., 2013 Global molecular epidemiology of Cryptococcus neoformans and
640 Cryptococcus gattii : An atlas of the molecular types. Scientifica 2013: 1–23.
641 https://doi.org/10.1155/2013/675213
642 Comeault A. A., and D. R. Matute, 2018 Genetic divergence and the number of hybridizing
643 species affect the path to homoploid hybrid speciation. PNAS 115: 9761–9766.
644 https://doi.org/10.1073/pnas.1809685115
645 Datta A., M. Hendrix, M. Lipsitch, and S. Jinks-Robertson, 1997 Dual roles for DNA sequence
646 identity and the mismatch repair system in the regulation of mitotic crossing-over
647 in yeast. Proc Natl Acad Sci U S A 94: 9757–9762.
648 Davidson R. C., M. C. Cruz, R. A. Sia, B. Allen, J. A. Alspaugh, *et al.*, 2000 Gene disruption by
649 biolistic transformation in serotype D strains of Cryptococcus neoformans. Fungal Genet
650 Biol 29: 38–48. https://doi.org/10.1006/fgbi.1999.1180

651 Dittrich-Reed D. R., and B. M. Fitzpatrick, 2013 Transgressive Hybrids as Hopeful Monsters.
652 Evol Biol 40: 310–315. https://doi.org/10.1007/s11692-012-9209-0
653 Dong K., M. You, and J. Xu, 2020 Genetic changes in experimental populations of a hybrid in
654 the Cryptococcus neoformans species complex. Pathogens 9: 3.
655 https://doi.org/10.3390/pathogens9010003
656 Ene L. V., R. A. Farrer, M. P. Hirakawa, K. Agwamba, C. A. Cuomo, *et al.*, 2018 Global analysis
657 of mutations driving microevolution of a heterozygous diploid fungal pathogen. Proc.
658 Natl. Acad. Sci. U. S. A. 115: E8688–E8697. https://doi.org/10.1073/pnas.1806002115
659 Fisher K. J., S. W. Buskirk, R. C. Vignogna, D. A. Marad, and G. I. Lang, 2018 Adaptive
660 genome duplication affects patterns of molecular evolution in Saccharomyces
661 cerevisiae. Plos Genetics 14: e1007396. https://doi.org/10.1371/journal.pgen.1007396
662 Forche A., J. Xu, R. Vilgalys, and T. G. Mitchell, 2000 Development and characterization of a
663 genetic linkage map of Cryptococcus neoformans var. neoformans using amplified
664 fragment length polymorphisms and other markers. Fungal Genet Biol 31: 189–203.
665 https://doi.org/10.1006/fgbi.2000.1240
666 Gabriel W., M. Lynch, and R. Bürger, 1993 Muller's ratchet and mutational meltdowns. Evolution
667 47: 1744–1757. https://doi.org/10.1111/j.1558-5646.1993.tb01266.x
668 Geissmann Q., 2013 OpenCFU, a new free and open-source software to count cell colonies and
669 other circular objects. PLOS ONE 8: e54072.
670 https://doi.org/10.1371/journal.pone.0054072
671 Gostinčar C., J. E. Stajich, J. Zupančič, P. Zalar, and N. Gunde-Cimerman, 2018 Genomic
672 evidence for intraspecific hybridization in a clonal and extremely halotolerant yeast. BMC
673 Genomics 19: 364. https://doi.org/10.1186/s12864-018-4751-5
674 Hu G. G., I. Liu, A. Sham, J. E. Stajich, F. S. Dietrich, *et al.*, 2008 Comparative hybridization
675 reveals extensive genome variation in the AIDS-associated pathogen Cryptococcus
676 neoformans. Genome Biol. 9: 17. https://doi.org/10.1186/gb-2008-9-2-r41

677 Hum Y. F., and S. Jinks-Robertson, 2019 Mismatch recognition and subsequent processing
678 have distinct effects on mitotic recombination intermediates and outcomes in yeast.
679 Nucleic Acids Research 47: 4554–4568. https://doi.org/10.1093/nar/gkz126
680 James T. Y., L. A. Michelotti, A. D. Glasco, R. A. Clemons, R. A. Powers, *et al.*, 2019
681 Adaptation by Loss of Heterozygosity in Saccharomyces cerevisiae Clones Under
682 Divergent Selection. Genetics 213: 665–683.
683 https://doi.org/10.1534/genetics.119.302411
684 Janbon G., K. L. Ormerod, D. Paulet, E. J. Byrnes, V. Yadav, *et al.*, 2014 Analysis of the
685 genome and transcriptome of Cryptococcus neoformans var. grubii reveals complex
686 RNA expression and microevolution leading to virulence attenuation. PLoS Genet 10:
687 e1004261. https://doi.org/10.1371/journal.pgen.1004261
688 Kavanaugh L. A., J. A. Fraser, and F. S. Dietrich, 2006 Recent evolution of the human pathogen
689 Cryptococcus neoformans by intervarietal transfer of a 14-gene fragment. Mol. Biol.
690 Evol. 23: 1879–1890. https://doi.org/10.1093/molbev/msl070
691 Lengeler K. B., G. M. Cox, and J. Heitman, 2001 Serotype AD strains of Cryptococcus
692 neoformans are diploid or aneuploid and are heterozygous at the mating-type locus.
693 Infect. Immun. 69: 115–122.
694 Li W. J., A. F. Averette, M. Desnos-Ollivier, M. Ni, F. Dromer, *et al.*, 2012 Genetic diversity and
695 genomic plasticity of Cryptococcus neoformans AD hybrid strains. G3-Genes Genomes
696 Genetics 2: 83–97. https://doi.org/10.1534/g3.111.001255
697 Lin X. R., K. Nielsen, S. Patel, and J. Heitman, 2008 Impact of mating type, serotype, and ploidy
698 on the virulence of Cryptococcus neoformans. Infect. Immun. 76: 2923–2938.
699 https://doi.org/10.1128/iai.00168-08
700 Litvintseva A. P., X. Lin, I. Templeton, J. Heitman, and T. G. Mitchell, 2007 Many globally
701 isolated AD hybrid strains of Cryptococcus neoformans originated in Africa. PLoS
702 Pathog. 3: 1109–1117. https://doi.org/10.1371/journal.ppat.0030114

703 Loftus B. J., E. Fung, P. Roncaglia, D. Rowley, P. Amedeo, *et al.*, 2005 The genome of the
704 basidiomycetous yeast and human pathogen Cryptococcus neoformans. Science 307:
705 1321–1324. https://doi.org/10.1126/science.1103773
706 Mallet J., 2007 Hybrid speciation. Nature 446: 279–283. https://doi.org/10.1038/nature05706
707 Marcet-Houben M., and T. Gabaldón, 2015 Beyond the whole-genome duplication:
708 Phylogenetic evidence for an ancient interspecies hybridization in the baker's yeast
709 lineage. PLOS Biology 13: e1002220. https://doi.org/10.1371/journal.pbio.1002220
710 McDonald M. J., D. P. Rice, and M. M. Desai, 2016 Sex speeds adaptation by altering the
711 dynamics of molecular evolution. Nature 531: 233–236.
712 https://doi.org/10.1038/nature17143
713 McKenna A., M. Hanna, E. Banks, A. Sivachenko, K. Cibulskis, *et al.*, 2010 The Genome
714 Analysis Toolkit: A MapReduce framework for analyzing next-generation DNA
715 sequencing data. Genome Res. 20: 1297–1303. https://doi.org/10.1101/gr.107524.110
716 Mixão V., and T. Gabaldón, 2020 Genomic evidence for a hybrid origin of the yeast
717 opportunistic pathogen Candida albicans. BMC Biology 18: 48.
718 https://doi.org/10.1186/s12915-020-00776-6
719 Opperman R., E. Emmanuel, and A. A. Levy, 2004 The effect of sequence divergence on
720 recombination between direct repeats in Arabidopsis. Genetics 168: 2207–2215.
721 https://doi.org/10.1534/genetics.104.032896
722 Orr H. A., and M. Turelli, 2001 The evolution of postzygotic isolation: accumulating Dobzhansky-
723 Muller incompatibilities. Evolution 55: 1085–1094. https://doi.org/10.1111/j.0014-
724 3820.2001.tb00628.x
725 Park H.-S., E. W. L. Chow, C. Fu, E. J. Soderblom, M. A. Moseley, *et al.*, 2016 Calcineurin
726 targets involved in stress survival and fungal virulence. PLOS Pathogens 12: e1005873.
727 https://doi.org/10.1371/journal.ppat.1005873

728 Phadke S. S., C. J. Maclean, S. Y. Zhao, E. A. Mueller, L. A. Michelotti, *et al.*, 2018 Genome-
729 wide screen for Saccharomyces cerevisiae genes contributing to opportunistic
730 pathogenicity in an invertebrate model host. G3-Genes Genomes Genetics 8: 63–78.
731 https://doi.org/10.1534/g3.117.300245
732 Priest S. J., M. A. Coelho, V. Mixão, S. A. Clancey, Y. Xu, *et al.*, 2021 Factors enforcing the
733 species boundary between the human pathogens Cryptococcus neoformans and
734 Cryptococcus deneoformans. PLoS Genet 17: e1008871.
735 https://doi.org/10.1371/journal.pgen.1008871
736 Pryszcz L. P., T. Németh, E. Saus, E. Ksiezopolska, E. Hegedüsová, *et al.*, 2015 The genomic
737 aftermath of hybridization in the opportunistic pathogen Candida metapsilosis. Plos
738 Genetics 11: e1005626. https://doi.org/10.1371/journal.pgen.1005626
739 Quinlan A. R., and I. M. Hall, 2010 BEDTools: a flexible suite of utilities for comparing genomic
740 features. Bioinformatics 26: 841–842. https://doi.org/10.1093/bioinformatics/btq033
741 R_Core_Team, 2019 *R: A language and environment for statistical computing*. R Foundation for
742 Statistical Computing, Vienna, Austria. URL: http://www.R-project.org/.
743 Rhodes J., C. A. Desjardins, S. M. Sykes, M. A. Beale, M. Vanhove, *et al.*, 2017 Tracing genetic
744 exchange and biogeography of Cryptococcus neoformans var. grubii at the global
745 population level. Genetics 207: 327–346. https://doi.org/10.1534/genetics.117.203836
746 Rieseberg L. H., M. A. Archer, and R. K. Wayne, 1999 Transgressive segregation, adaptation
747 and speciation. Heredity 83: 363–372. https://doi.org/10.1038/sj.hdy.6886170
748 Rieseberg L. H., 2001 Polyploid evolution: Keeping the peace at genomic reunions. Current
749 Biology 11: R925–R928. https://doi.org/10.1016/S0960-9822(01)00556-5
750 Roth C., S. Sun, R. B. Billmyre, J. Heitman, and P. M. Magwene, 2018 A high-resolution map of
751 meiotic recombination in Cryptococcus deneoformans demonstrates decreased
752 recombination in unisexual reproduction. Genetics 209: 567–578.
753 https://doi.org/10.1534/genetics.118.300996

754 Saikkonen K., C. A. Young, M. Helander, and C. L. Schardl, 2016 Endophytic Epichloë species
755 and their grass hosts: from evolution to applications. Plant Mol. Biol. 90: 665–675.
756 https://doi.org/10.1007/s11103-015-0399-6
757 Samarasinghe H., and J. Xu, 2018 Hybrids and hybridization in the Cryptococcus neoformans
758 and Cryptococcus gattii species complexes. Infect. Genet. Evol. 66: 245–255.
759 https://doi.org/10.1016/j.meegid.2018.10.011
760 Samarasinghe H., M. You, T. S. Jenkinson, J. Xu, and T. Y. James, 2020a Hybridization
761 facilitates adaptive evolution in two major fungal pathogens. Genes (Basel) 11: 101.
762 https://doi.org/10.3390/genes11010101
763 Samarasinghe H., A. Vogan, N. Pum, and J. Xu, 2020b Patterns of allele distribution in a hybrid
764 population of the Cryptococcus neoformans species complex. Mycoses 63: 275–283.
765 https://doi.org/10.1111/myc.13040
766 Schardl C. L., and K. D. Craven, 2003 Interspecific hybridization in plant-associated fungi and
767 oomycetes: a review. Mol. Ecol. 12: 2861–2873. https://doi.org/10.1046/j.1365-
768 294X.2003.01965.x
769 Schröder M. S., K. M. de S. Vicente, T. H. R. Prandini, S. Hammel, D. G. Higgins, *et al.*, 2016
770 Multiple origins of the pathogenic yeast Candida orthopsilosis by separate hybridizations
771 between two parental species. PLOS Genetics 12: e1006404.
772 https://doi.org/10.1371/journal.pgen.1006404
773 Seplyarskiy V. B., M. D. Logacheva, A. A. Penin, M. A. Baranova, E. V. Leushkin, *et al.*, 2014
774 Crossing-over in a hypervariable species preferentially occurs in regions of high local
775 smilarity. Molecular Biology and Evolution 31: 3016–3025.
776 https://doi.org/10.1093/molbev/msu242
777 Serrato-Capuchina A., and D. R. Matute, 2018 The role of transposable elements in speciation.
778 Genes (Basel) 9: 254. https://doi.org/10.3390/genes9050254

779 Shapira R., T. Levy, S. Shaked, E. Fridman, and L. David, 2014 Extensive heterosis in growth of
780 yeast hybrids is explained by a combination of genetic models. Heredity 113: 316–326.
781 https://doi.org/10.1038/hdy.2014.33
782 St Charles J., E. Hazkani-Covo, Y. Yin, S. L. Andersen, F. S. Dietrich, *et al.*, 2012 High-
783 resolution genome-wide analysis of irradiated (UV and gamma-rays) diploid yeast cells
784 reveals a high frequency of genomic loss of heterozygosity (LOH) events. Genetics 190:
785 1267–1284. https://doi.org/10.1534/genetics.111.137927
786 Steen B. R., S. Zuyderduyn, D. L. Toffaletti, M. Marra, S. J. M. Jones, *et al.*, 2003 Cryptococcus
787 neoformans gene expression during experimental cryptococcal meningitis. Eukaryotic
788 Cell 2: 1336–1349. https://doi.org/10.1128/EC.2.6.1336-1349.2003
789 Steenwyk J. L., A. L. Lind, L. N. A. Ries, T. F. dos Reis, L. P. Silva, *et al.*, 2020 Pathogenic
790 allodiploid hybrids of Aspergillus fungi. Current Biology 30: 2495-2507.e7.
791 https://doi.org/10.1016/j.cub.2020.04.071
792 Stone N. R. H., J. Rhodes, M. C. Fisher, S. Mfinanga, S. Kivuyo, *et al.*, 2019 Dynamic ploidy
793 changes drive fluconazole resistance in human cryptococcal meningitis. J Clin Invest
794 129: 999–1014. https://doi.org/10.1172/JCI124516
795 Stukenbrock E. H., 2016 The role of hybridization in the evolution and emergence of new fungal
796 plant pathogens. Phytopathology 106: 104–112. https://doi.org/10.1094/phyto-08-15-
797 0184-rvw
798 Sui Y., L. Qi, J.-K. Wu, X.-P. Wen, X.-X. Tang, *et al.*, 2020 Genome-wide mapping of
799 spontaneous genetic alterations in diploid yeast cells. PNAS 117: 28191–28200.
800 https://doi.org/10.1073/pnas.2018633117
801 Sun S., and J. P. Xu, 2007 Genetic analyses of a hybrid cross between serotypes A and D
802 strains of the human pathogenic fungus Cryptococcus neoformans. Genetics 177: 1475–
803 1486. https://doi.org/10.1534/genetics.107.078923

804 Sun S., and J. Xu, 2009 Chromosomal rearrangements between serotype A and D strains in
805 Cryptococcus neoformans. PLoS ONE 4: e5524.
806 Sun S., R. B. Billmyre, P. A. Mieczkowski, and J. Heitman, 2014 Unisexual reproduction drives
807 meiotic recombination and phenotypic and karyotypic plasticity in Cryptococcus
808 neoformans. PLOS Genetics 10: e1004849.
809 https://doi.org/10.1371/journal.pgen.1004849
810 Symington L. S., R. Rothstein, and M. Lisby, 2014 Mechanisms and regulation of mitotic
811 recombination in Saccharomyces cerevisiae. Genetics 198: 795–835.
812 https://doi.org/10.1534/genetics.114.166140
813 Tattini L., N. Tellini, S. Mozzachiodi, M. D'Angiolo, S. Loeillet, *et al.*, 2019 Accurate tracking of
814 the mutational landscape of diploid hybrid genomes. Molecular Biology and Evolution 36:
815 2861–2877. https://doi.org/10.1093/molbev/msz177
816 Torres M. P., F. Entwistle, and P. J. Coote, 2016 Effective immunosuppression with
817 dexamethasone phosphate in the Galleria mellonella larva infection model resulting in
818 enhanced virulence of Escherichia coli and Klebsiella pneumoniae. Med Microbiol
819 Immunol 205: 333–343. https://doi.org/10.1007/s00430-016-0450-5
820 Treangen T. J., B. D. Ondov, S. Koren, and A. M. Phillippy, 2014 The Harvest suite for rapid
821 core-genome alignment and visualization of thousands of intraspecific microbial
822 genomes. Genome Biology 15: 524. https://doi.org/10.1186/s13059-014-0524-x
823 Vogan A. A., and J. Xu, 2014 Evidence for genetic incompatibilities associated with post-zygotic
824 reproductive isolation in the human fungal pathogen Cryptococcus neoformans. Genome
825 57: 335–344. https://doi.org/10.1139/gen-2014-0077
826 Vogan A. A., J. Khankhet, H. Samarasinghe, and J. P. Xu, 2016 Identification of QTLs
827 associated with virulence related traits and drug resistance in Cryptococcus neoformans.
828 G3-Genes Genomes Genet. 6: 2745–2759. https://doi.org/10.1534/g3.116.029595
829 Wickham H., 2009 *ggplot2: Elegant Graphics for Data Analysis*. Springer-Verlag, New York.

830 Xu J., A. R. Ramos, R. Vilgalys, and T. G. Mitchell, 2000a Clonal and spontaneous origins of
831 fluconazole resistance in Candida albicans. J Clin Microbiol 38: 1214–1220.
832 https://doi.org/10.1128/JCM.38.3.1214-1220.2000
833 Xu J., R. Vilgalys, and T. G. Mitchell, 2000b Multiple gene genealogies reveal recent dispersion
834 and hybridization in the human pathogenic fungus Cryptococcus neoformans. Mol. Ecol.
835 9: 1471–1481. https://doi.org/10.1046/j.1365-294x.2000.01021.x
836 Xu J. P., G. Z. Luo, R. J. Vilgalys, M. E. Brandt, and T. G. Mitchell, 2002 Multiple origins of
837 hybrid strains of Cryptococcus neoformans with serotype AD. Microbiology-(UK) 148:
838 203–212.
839 Yang D.-H., K.-W. Jung, S. Bang, J.-W. Lee, M.-H. Song, *et al.*, 2017 Rewiring of signaling
840 networks modulating thermotolerance in the human pathogen Cryptococcus
841 neoformans. Genetics 205: 201–219. https://doi.org/10.1534/genetics.116.190595
842 Yu G., L.-G. Wang, Y. Han, and Q.-Y. He, 2012 clusterProfiler: an R package for comparing
843 biological themes among gene clusters. OMICS 16: 284–287.
844 https://doi.org/10.1089/omi.2011.0118
845 Zanders S. E., M. T. Eickbush, J. S. Yu, J.-W. Kang, K. R. Fowler, *et al.*, 2014 Genome
846 rearrangements and pervasive meiotic drive cause hybrid infertility in fission yeast. Elife
847 3: e02630. https://doi.org/10.7554/eLife.02630
848 Zhu Y. O., G. Sherlock, and D. A. Petrov, 2016 Whole genome analysis of 132 clinical
849 Saccharomyces cerevisiae strains reveals extensive ploidy variation. G3-Genes
850 Genomes Genet. 6: 2421–2434. https://doi.org/10.1534/g3.116.029397/-/DC1
851

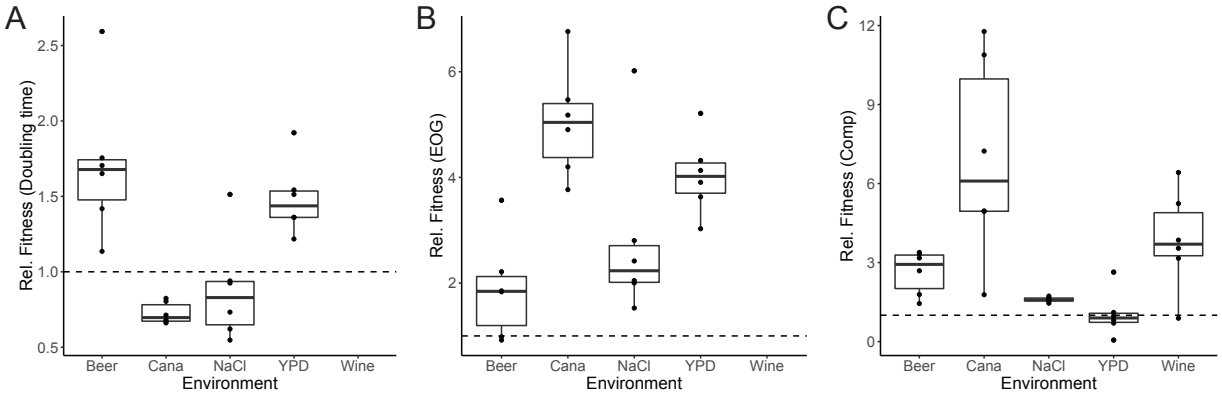

Figure 1. Clones evolved in *in vitro* conditions mostly showed fitness gains regardless of means of estimation. Shown are values of relative fitness comparing a clone grown in the same media in which evolution occurred relative to the fitness of the ancestral genotype SSD-719 (dashed line). A) Fitness measured using doubling time. B) Fitness measured using EOG = Efficiency of Growth (i.e., carrying capacity). C) Fitness measured using relative competitive growth in the presence of a marked ancestral strain. Each dot represents an individual clone. Boxes indicate the 25-75% percentiles, bars indicate medians, and the whiskers extend to 1.5 x the interquartile range. Wine strains were not tested by growth curve analysis due to opacity of the medium.

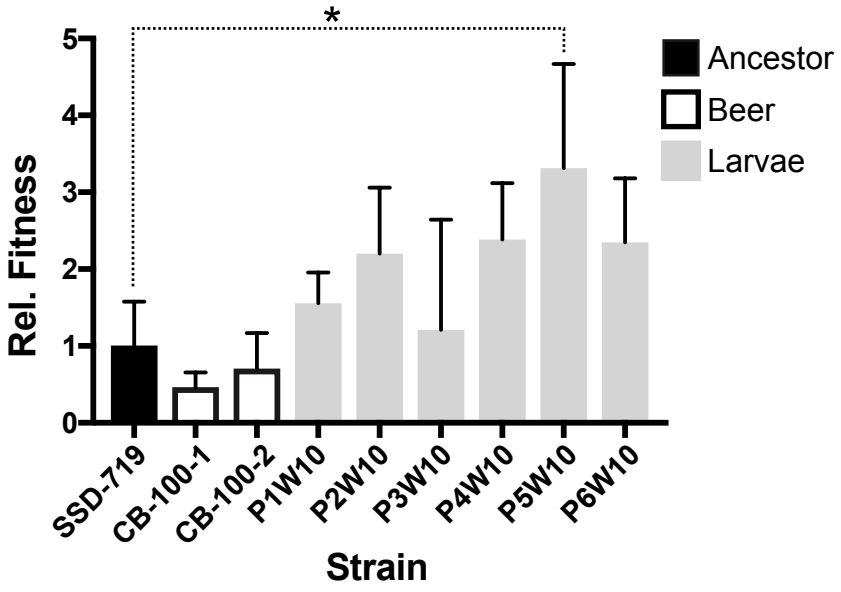

Figure 2. Strains passaged in larvae showed overall greater fitness than the ancestor as measured by recovery after 2 days growth post-coinjection with a common competitor strain (SSE-761). Three replicate experiments were conducted for each strain, and values indicate mean (+1 sd). All values are shown relative to the fitness of SSD-719 (ancestor) which was set to 1.0. Post-Hoc comparisons of the fitness between each evolved strain and the ancestor via by Fisher's LSD found only the difference between SSD-719 and P5W10 to be significant (P=0.0039). P4W10 and P6W10 were marginally significantly different from SSD-719 (P=0.06 and P=0.07, respectively).

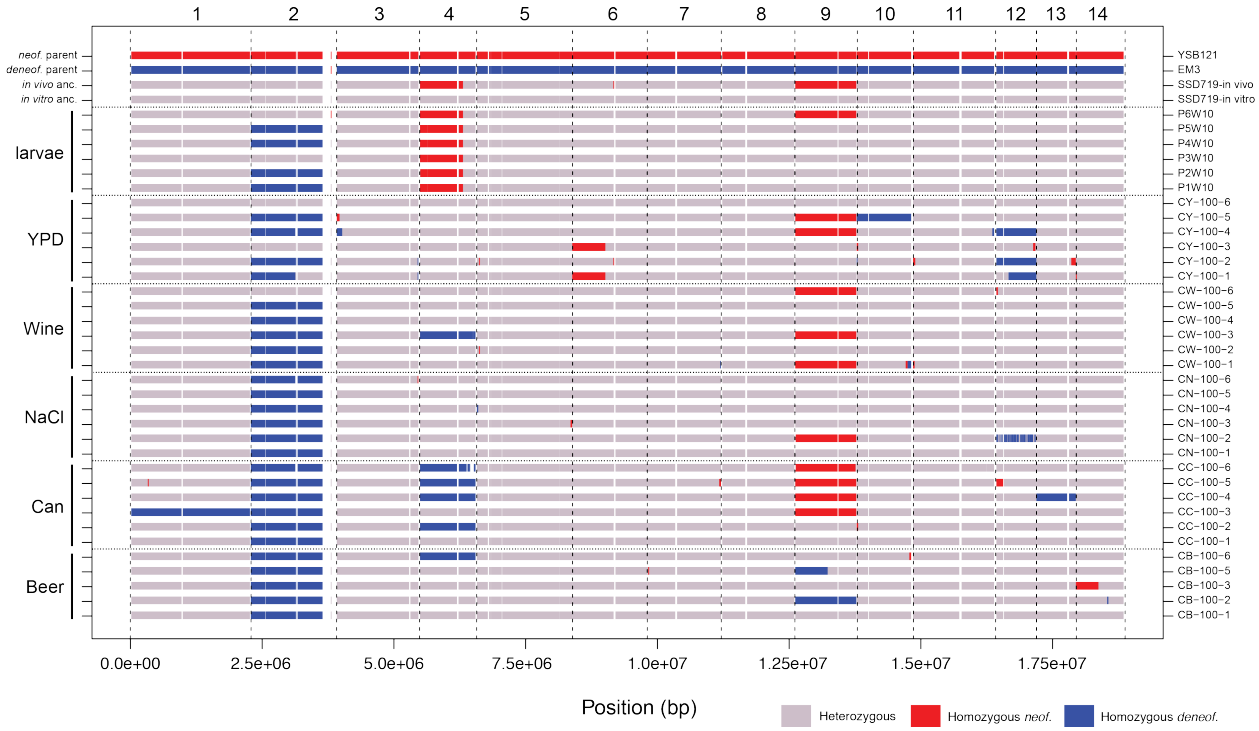

Figure 3. Landscape of LOH across the 14 chromosomes of the evolved clones. Shown are genotypes at 10 kb resolution of the strains, with media type shown on the left margin and strain name on the right margin. The ancestral genotype of the *in vivo* (larval) passaging was different from the *in vitro* (other media types), because the experiments began at different times. The reference genome coordinates are from the *C. neoformans* parent. White regions represent unmapped, typically repetitive regions of the genome, or for the right arm of Chr 2 a LOH event that occurred in the ancestor before passaging.

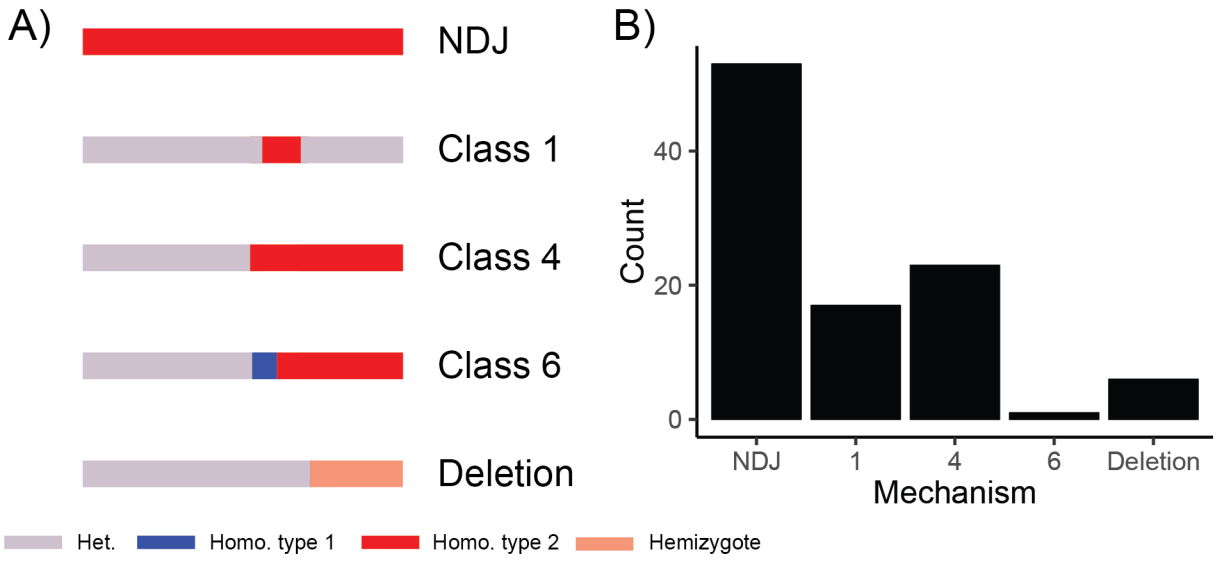

Figure 4. Summary of detected LOH mechanisms across the 35 evolved hybrid clones. (A) A depiction of proposed LOH mechanisms according to schema defined by St. Charles (St Charles *et al.* 2012), and (B) Tallied numbers of events observed among the hybrid clones.

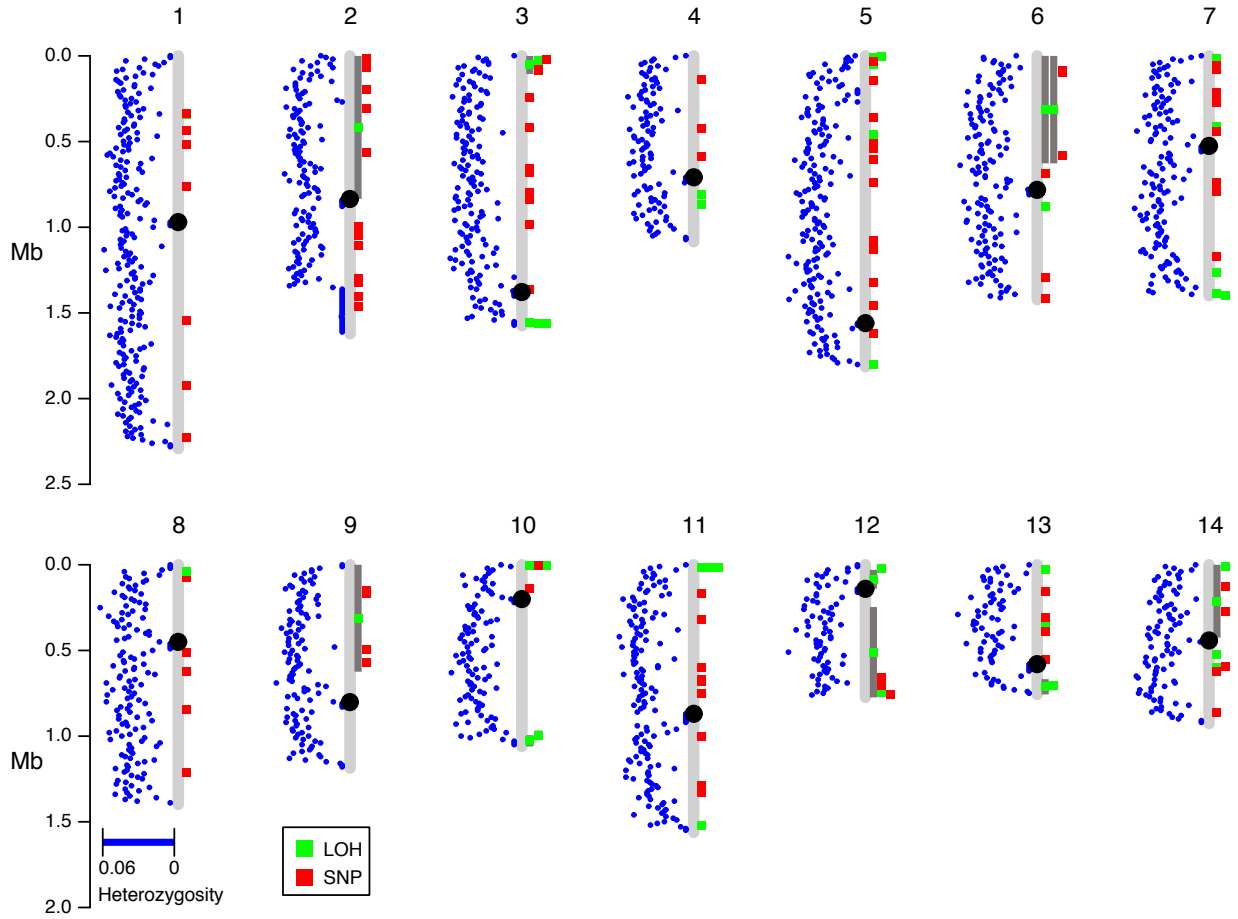

Figure 5. Locations of mitotic recombination breakpoints are non-random across the genome. Blue dots indicate the average heterozygosity in 10 kb windows between *C. neoformans* and *C. deneoformans* parental genomes that passed our filtering strategies. Dark grey bars indicate LOH tracts.

Suppl. Table 1. Markers used for screening mating products for heterozygosity. Chromosome numbers and positions are relative to the H99 genome.

Marker	Chromosome	Position	Forward Primer (5' - 3')	Reverse Primer (5' - 3')
Chrom01_Region5	1	128800-131200	GCACATGAAGAAATATGACCG	GCACATTCGCCAATCCTATC
Chrom01_Region8	1	389600-391200	AATGAGACGAATACGGTCGG	AGCTCTCTTTCACTGACACGA
Chrom02_Region1	2	88000-89600	GCACAGGCCAGTAAAGGAGG	GAATCTGAGAAGGCTGAGGCTA
Chrom02_Region5	2	1228800-1231200	GCTGCTGCATTTGCTGAG	TGAAATGAACGAACTAGTACGG
Chrom07_Region1	7	56800-59200	CGCCCTCTTGCTGAAGTTG	TTTCTCTTGTGCTTCAAATGC
Chrom07_Region5	7	512800-514400	GAAATGGTGCGAGAATAGGC	CATCTGCACTTCGAACGAC
Chrom10_Region7	10	967200-968000	ATTTTCAGGTATCCCCATGC	CATTGGTAAACTCGCCTCTG
Chrom12_Region1	12	87200-88800	GGAACGAGATGGAAATCGG	GTCTCACTGCCAGTAAAGTCAG
Chrom12_Region8	12	721600-724000	GCCATTTGGACTTTGGGTG	TGACTCTTGTGGAGCTTAACG
Chrom13_Region1	13	108000-108800	CGCCTTTGATTGCTGATGAC	GGGATAGCTCTTGGCAATGC
Chrom13_Region4	13	693600-695200	GAAGCCATCTTGCTGAAGTG	TTCGGGAGGGTGACTCTC
STE20_neo_MATalpha	5	247512-247841	GGCTGCAATCACAGCACCTTAC	CTTCATGACATCACTCCCCTAT
STE20_deneo_MATa	5	n.a.	CACATCTCAGATGCCATTTTACCA	AGCTCTAAGTCATATGGGTTATAT

Suppl. Table 2. Heterozygosity is not correlated with frequency of crossover events or aneuploidy at the whole chromosome level. Data are relative to *C. neoformans* H99 genome. Only one breakpoint for each gene conversion is considered.

Chr	Size	Num SNPs	SNP rate	Num. breaks	Aneuploidies
1	2291499	72959	0.0318	1	1
2	1621675	39814	0.0246	1	29
3	1575141	50117	0.0318	5	6
4	1084805	30247	0.0279	2	0
5	1814975	54199	0.0299	6	0
6	1422463	45598	0.0321	3	0
7	1399503	42668	0.0305	7	0
8	1398693	42582	0.0304	1	0
9	1186808	37586	0.0317	1	12
10	1059964	29439	0.0278	5	1
11	1561994	47038	0.0301	4	0
12	774062	20441	0.0264	4	3
13	756744	20401	0.0270	3	1
14	926563	27207	0.0294	4	0

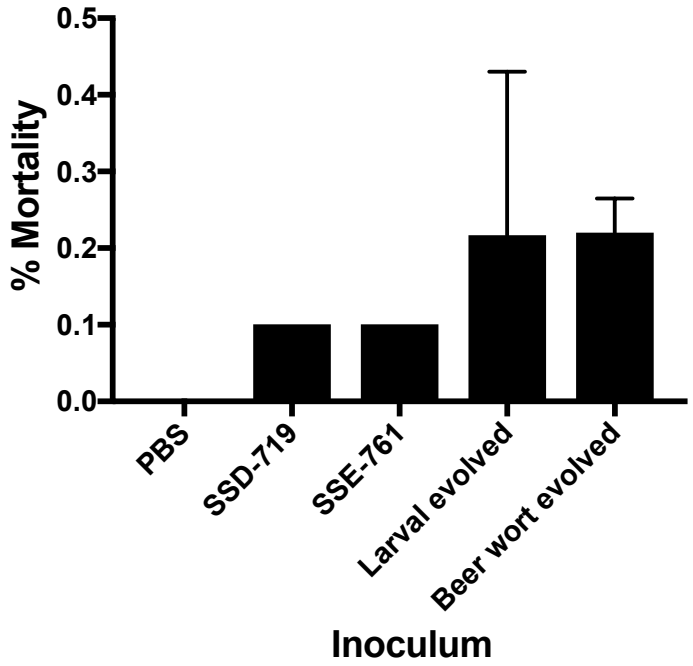

Suppl. Figure 1. Strains evolved in both larvae and beer show similar virulence as measured by *G. mellonella* survival 5 days post inoculation. Each strain was inoculated into 10 larvae and monitored for survival for up to 1 week. Values and error bars for evolved strains are means and SD for 5-6 independently evolved genotypes. Only one replicate was done for the two ancestral genotypes (SSD-719 and SSE-761) and the cell-free control (PBS). By 7 dpi values were qualitatively similar and most infected animals had died.

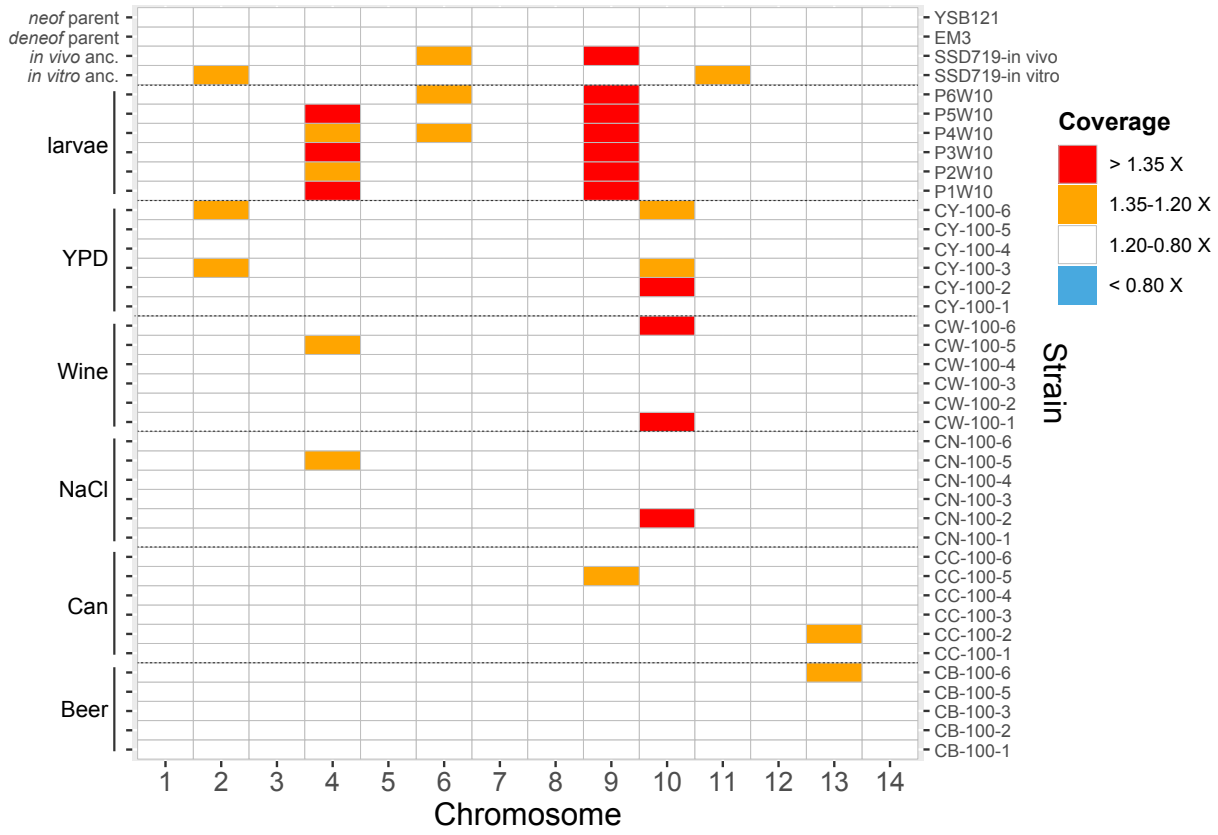

Suppl. Figure 2. Heatmap of chromosome-level coverage indicates aneuploidy in both ancestral strains and evolved strains. Relative coverage to genome-wide mean is indicated. No chromosomes had less than 0.8 X coverage.

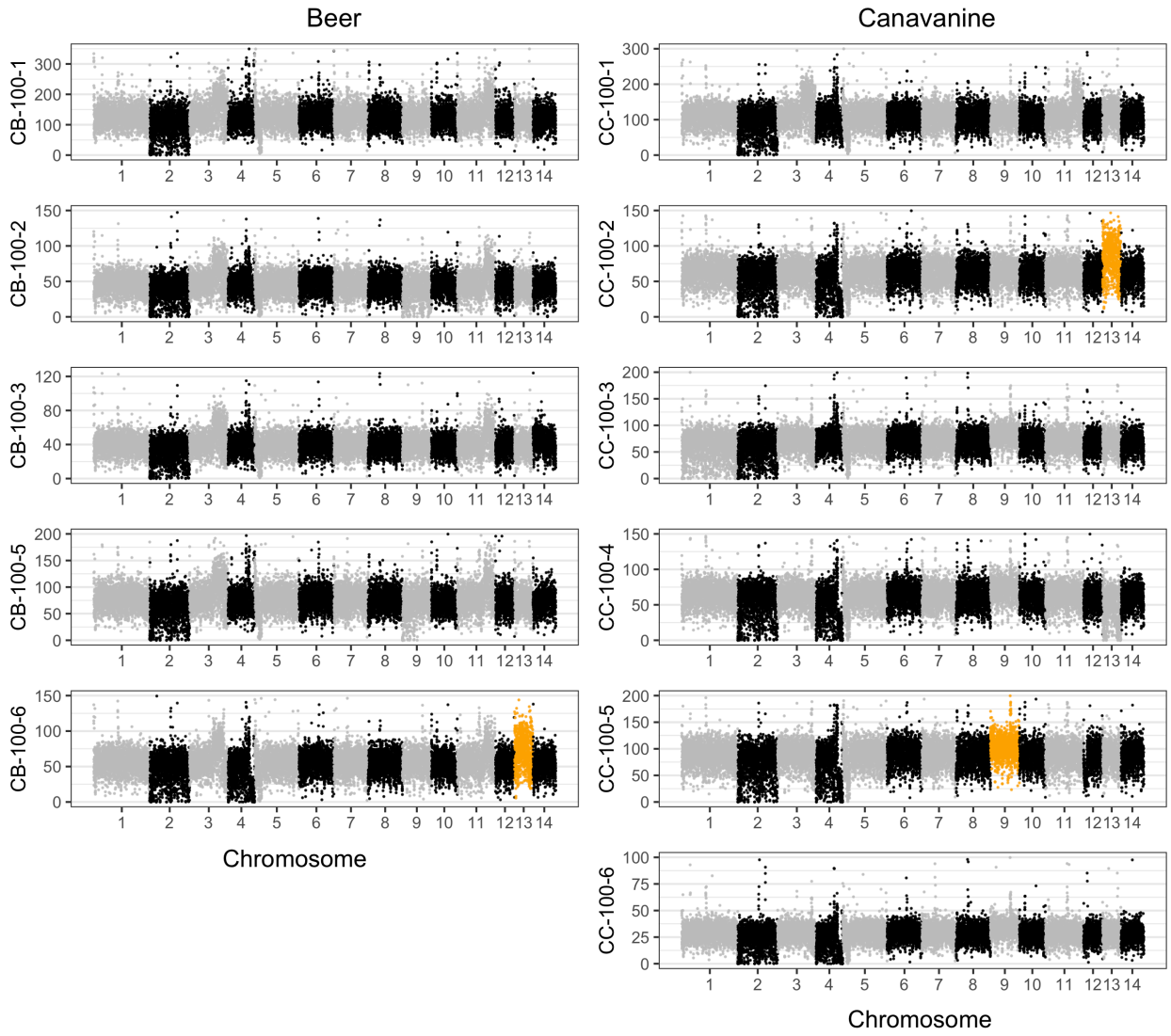

Suppl. Figure 3. Coverage of strains evolved in beer wort and canavanine media across the 14 chromosomes (*C. neoformans* reference genome) at 1 kb resolution. Points plotted in orange are for chromosomes with >1.2X genome-wide coverage mean, and red points indicate >1.35X genome-wide coverage mean.

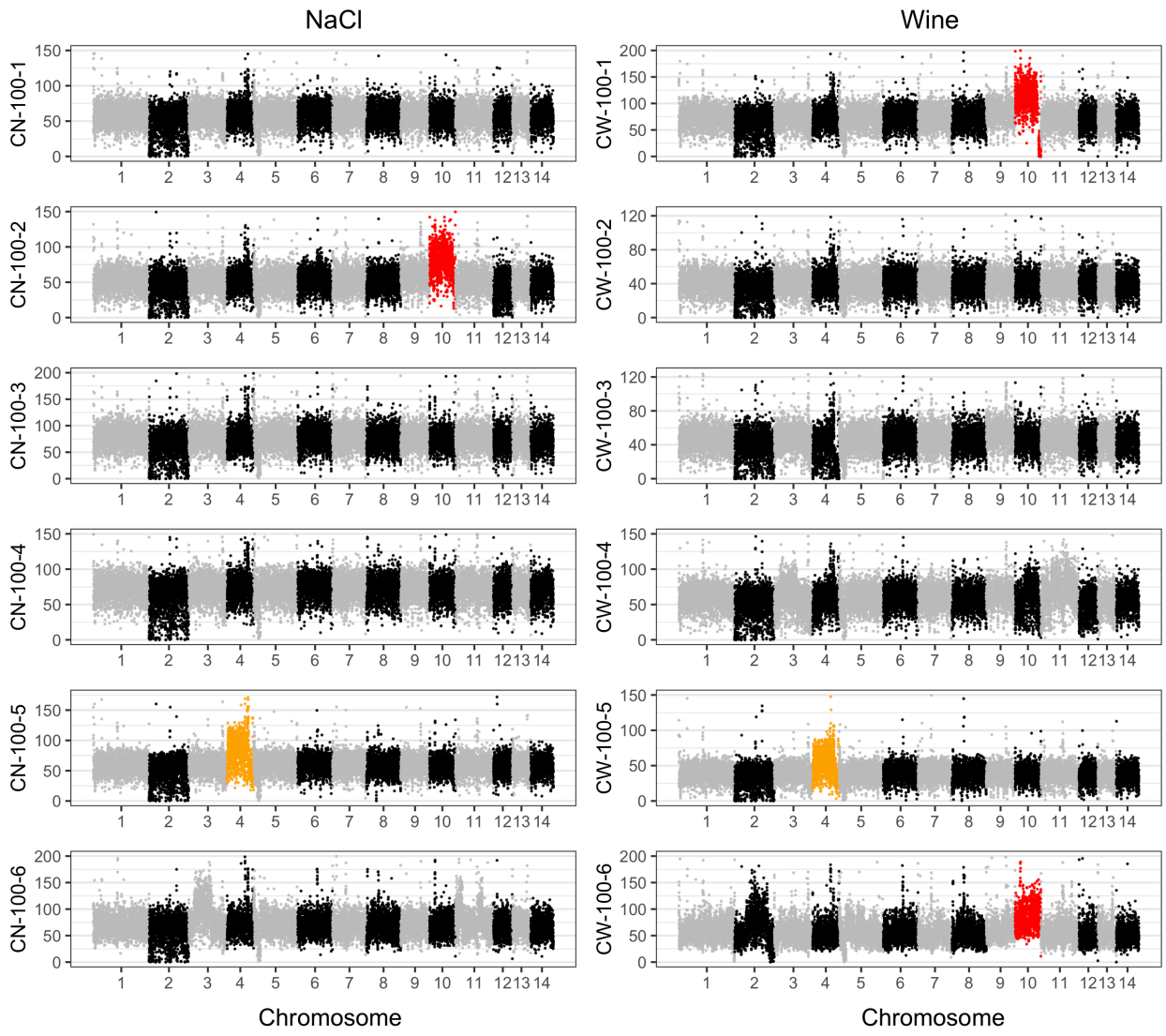

Suppl. Figure 4. Coverage of strains evolved in high salt and wine must media across the 14 chromosomes (*C. neoformans* reference genome) at 1 kb resolution. Points plotted in orange are for chromosomes with >1.2X genome-wide coverage mean, and red points indicate >1.35X genome-wide coverage mean.

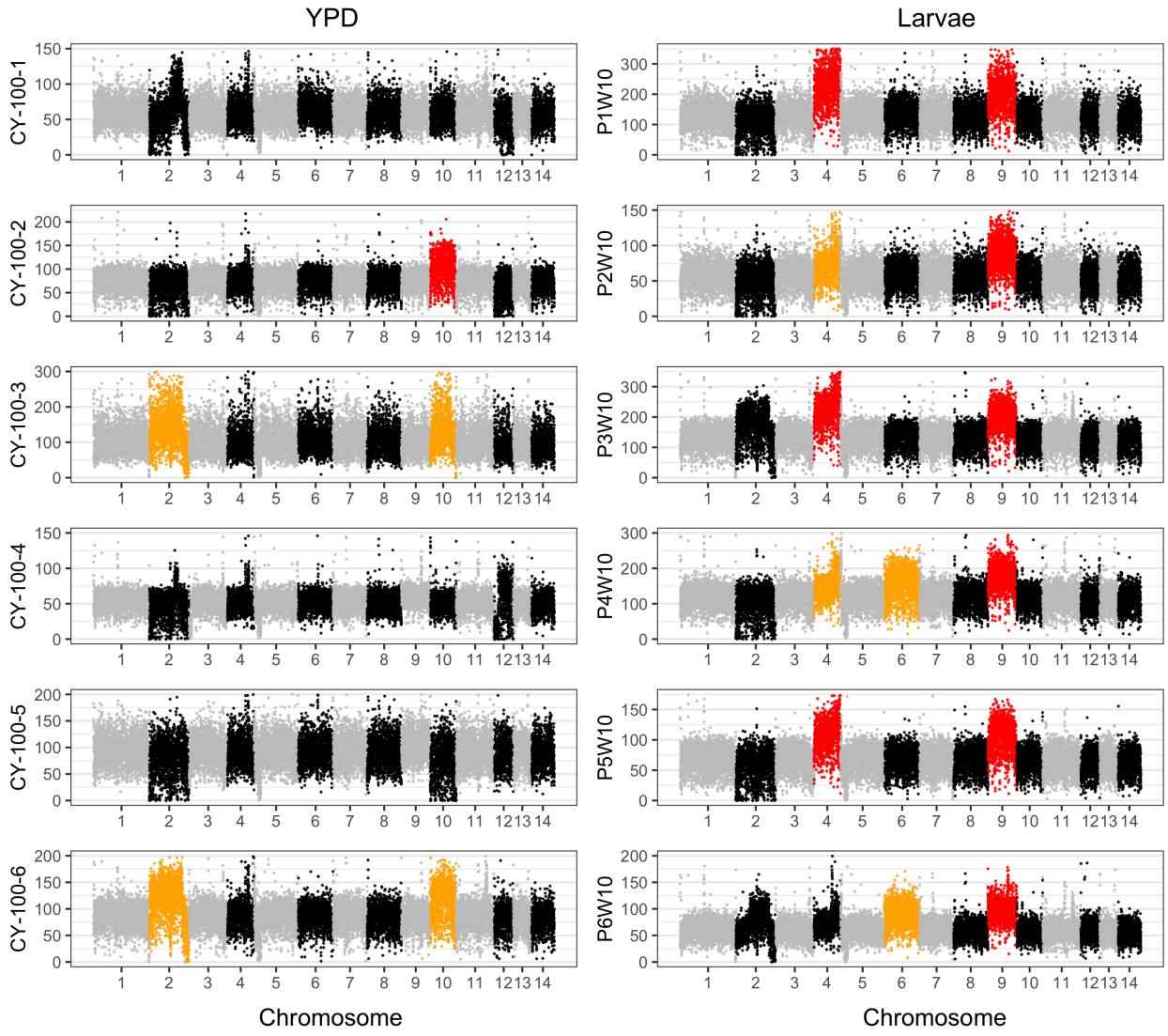

Suppl. Figure 5. Coverage of strains evolved in YPD and *G. mellonella* across the 14 chromosomes (*C. neoformans* reference genome) at 1 kb resolution. Points plotted in orange are for chromosomes with >1.2X genome-wide coverage mean, and red points indicate >1.35X genome-wide coverage mean.

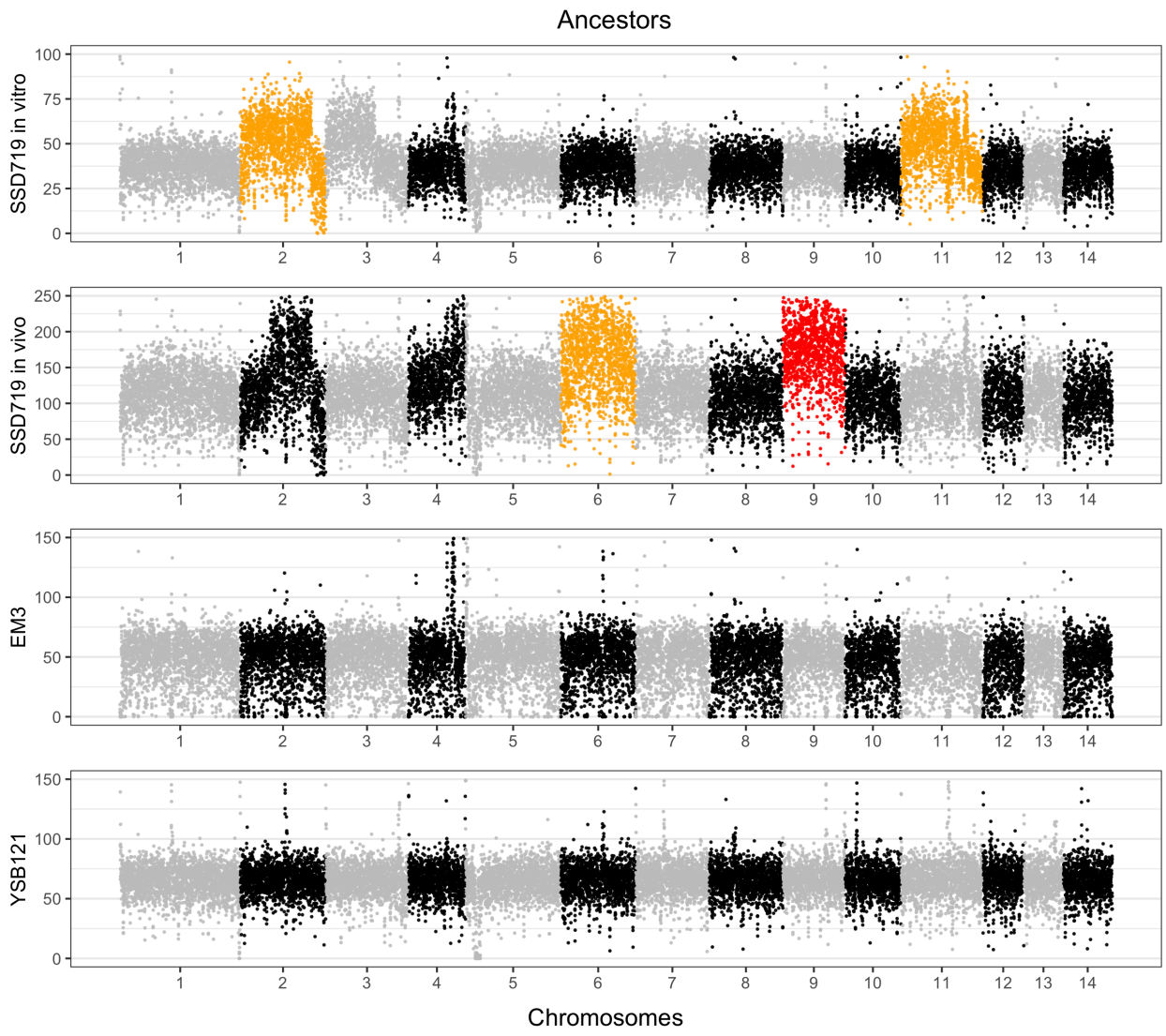

Suppl. Figure 6. Coverage of ancestral diploid (SSD719-*in vitro* and SSD719-*in vivo*) and haploid (EM3 and YSB121) genotypes across the 14 chromosomes (*C. neoformans* reference genome) at 1 kb resolution. Points plotted in orange are for chromosomes with >1.2X genome-wide coverage mean, and red points indicate >1.35X genome-wide coverage mean.